

國立交通大學

電子工程學系 電子研究所碩士班

碩士論文

適用於 MIMO OFDM 系統之 V-BLAST 偵測技術的研究  
與其改善設計



Investigation of V-BLAST Detection Technique and Its  
Improvement for MIMO OFDM Systems

研究生：張譽桀

指導教授：陳紹基 博士

中華民國九十五年八月

適用於 MIMO OFDM 系統之 V-BLAST 偵測技術的研  
究與其改善設計

Investigation of V-BLAST Detection Technique and Its  
Improvement for MIMO OFDM Systems

研究生：張譽桀

Student：Yu-Chieh Chang

指導教授：陳紹基 博士

Advisor：Sau-Gee Chen

國立交通大學

電子工程學系 電子研究所碩士班



Submitted to Department of Electronics Engineering & Institute of Electronics

College of Electrical Engineering and Computer Science

National Chiao Tung University

in partial Fulfillment of the Requirements

for the Degree of

Master

in

Electronics Engineering

July 2006

Hsinchu, Taiwan, Republic of China

中華民國九十五年八月

# 適用於 MIMO OFDM 系統之 V-BLAST 偵測技術的研究與其改善設計

學生：張譽桀

指導教授：陳紹基 博士

國立交通大學

電子工程學系 電子研究所碩士班

## 摘 要

本論文討論 MIMO-OFDM 訊號偵測的相關技術，特別是 V-BLAST 技術。還有介紹各種關於 V-BLAST 演算法的變化技術，依效能不同有高複雜度也有低複雜度，我們提出新的 MIMO-OFDM 訊號偵測演算法首先簡化最大可能性技術(ML)大量的複雜度並結合此簡化之 ML 技巧和 V-BLAST 以兼顧複雜度與效能表現。經由複雜度比較和位元錯誤率(BER)效能模擬，結果顯示我們提出的演算法性能比 V-BLAST 好並且只會增加一小部分的複雜度。

# Investigation of V-BLAST Detection Technique and Its Improvement for MIMO OFDM Systems

Student: Yu-Chieh Chang

Advisor: Sau-Gee Chen

Department of Electronics Engineering & Institute of Electronics  
National Chiao Tung University

## Abstract



In this thesis, signal detection techniques for MIMO OFDM systems are investigated, particularly the V-BLAST technique. In addition, all the enhanced and modified detection methods based on V-BLAST are studied. Those techniques may have higher or lower complexities than V-BLAST technique, depending on their performance. In order to achieve high-performance detection with low complexities we propose a new detection algorithm by combining a simplified maximum likelihood method with V-BLAST detection. Simulation results and complexity comparisons show the proposed methods achieve better performances than the conventional method at the cost of small complexities.

# 誌謝

---

在這兩年之中我的指導教授陳紹基博士，對我們的課業研究方向提供了很多幫助在這兩年中對於我的課業研究著實提供了許多幫助，除了他扎實的知識，還有遊歷過不少國家的趣聞，都是值得我再三回味，在此獻上由衷的感激。

此外要感謝的是實驗室 429 的同學們，在課業上提供我不少的幫助，可以談心說地，並且在生活上互相幫助，在這不短不長的兩年研究所生涯之中，很高興能夠有金融、昀震、文威、敏杰的陪伴，也祝福他們在未來的人生之中能夠發揮在這裡學到的東西，並且迎向燦爛的人生；建全學長也給了我們關於課業還有未來工作上面的建議，讓我們對未來有更進一步的認知，而不再感到惶恐，在此由衷的感激，在快要離開交大的這個時刻，希望以後大家能夠固定時間約出來聊聊近況。

最後，要感謝我的父母，給我很多包容還有經濟上的支柱，使得我能夠平安順利的完成學業，謝謝。

# Contents

中文摘要.....	I
ABSTRACT.....	II
誌謝.....	III
CONTENTS.....	IV
LIST OF TABLES .....	VI
LIST OF FIGURES .....	VII
<b>Chapter 1 Introduction</b> .....	<b>1</b>
1.1 Background.....	1
1.2 Motivations .....	2
1.3 Organization of the Thesis .....	3
<b>Chapter 2 OFDM and MIMO Fundamentals</b> .....	<b>4</b>
2.1 OFDM System Models .....	4
2.1.1 Continuous Time Model .....	5
2.1.2 Discrete Time Model.....	7
2.1.3 Effect of Cyclic Prefix .....	8
2.2 Concept of Multiple-Input Multiple-Output (MIMO) Systems.....	8
2.2.1 MIMO System Model.....	9
2.2.2 MIMO-OFDM Architecture.....	11
2.2.3 An example MIMO OFDM System EWC 802.11n.....	12
2.3 Signal Detection Algorithms for MIMO Systems .....	15
2.3.1 Maximum-Likelihood (ML) Detection.....	16
2.3.2 V-BLAST Detection Method .....	16
2.3.3 Detection Methods based on V-BLAST .....	18
2.3.3.1 Simplified V-BLAST Detection.....	18
2.3.3.2 Enhanced V-BLAST Detection.....	20
2.3.3.2.1 Two Iterative V-BLAST Detection Algorithms .....	20
2.3.3.2.2 Enhanced Zero-Forcing V-BLAST Detection.....	25
2.3.3.2.3 Joint ML and DFE Scheme for V-BLAST .....	27
2.3.3.3 The MMSE-BLAST Detection Method.....	28
2.3.3.3.1 Modified Channel Matrix on the MMSE V-BLAST Technique .....	29
2.3.3.4 V-BLAST Technique with Parallel Symbol Cancellation.....	30
2.3.3.4.1 Two-Stage V-BLAST Detection Algorithm .....	30

2.3.4 Comparisons of Data Detection Algorithms .....	32
<b>Chapter 3 The Proposed Data Detection Algorithms</b>	<b>35</b>
3.1 The New Detection Methods .....	35
3.1.1 New Hybrid ML and V-BLAST Detection Method.....	36
3.1.2 Extension of the new method.....	38
3.2 The Compared Detection Techniques .....	39
3.3 Reducing Computational Complexities in Pseudo-Inverse .....	40
3.4 Complexity Analysis and Comparison.....	41
<b>Chapter 4 Simulation Results</b>	<b>45</b>
4.1 Performance – Execution Time.....	46
4.2 Performance – Bit Error Rate .....	49
<b>Chapter 5 Conclusion</b>	<b>64</b>
<b>Bibliography</b>	<b>65</b>



## List of Tables

---

Table 2.1 Parameters and specifications of EWC 802.11n systems [11]	13
Table 2.2 Change of diversity degree in each V-BLAST's loop [19]	21
Table 2.3 Number of pseudoinverses of the Li's and Shen's approaches [21]	24
Table 2.4 Complexity comparisons of data detection algorithms	33
Table 3.1 Multiplication complexities of various detection algorithms without considering matrix symmetry	42
Table 3.2 Multiplication complexities of various detection algorithms, considering matrix symmetry	43
Table 4.1 Simulated EWC system parameters	46
Table 4.2 Multiplication complexities of the proposed detection algorithms vs. L value, considering matrix symmetry	48
Table 4.3 Indoor channel model [28] with short delays, office environment	49
Table 4.4 Indoor channel model [28], large hall environment	56





## List of Figures

Figure 2.1 Cyclic prefix of an OFDM symbol [18]	5
Figure 2.2 Spectrum of an OFDM signal [18]	6
Figure 2.3 (a) Continuous-time OFDM baseband modulator [18]	6
Figure 2.3 (b) Continuous-time OFDM baseband demodulator [18]	6
Figure 2.4 Discrete-time OFDM system model [18]	7
Figure 2.5 Wireless MIMO transmission model [17]	10
Figure 2.6 Transmitter architecture of a MIMO OFDM system [10]	11
Figure 2.7 Receiver architecture of a MIMO OFDM system [10]	12
Figure 2.8 PLCP frame format of EWC 802.11n standard [12]	14
Figure 2.9 Cyclical delay format of the preamble in EWC 802.11n standard [11]	15
Figure 2.10 The 0 <sup>th</sup> -order simplified V-BLAST detection algorithm in [13]	18
Figure 2.11 The simplified V-BLAST detection algorithm in [18]	19
Figure 2.12 Li's iterative V-BLAST detection algorithm	24
Figure 2.13 Equation (2.16) as function of $\ \hat{n}\ $ [22]	25
Figure 2.14 Equation (2.17) as function of $\ \hat{n}\ $ [22]	26
Figure 2.15 ML detection equation (number of transmitter antennas = $N_t$ )	27
Figure 2.16 ML detection equation (number of transmitter antennas = $p$ )	27
Figure 3.1 The proposed hybrid ML and V-BLAST detection	37
Figure 3.2 The proposed hybrid ML and V-BLAST detection (simplest case for $L = 1$ )	37
Figure 3.3 Flow diagram of the proposed hybrid ML and V-BLAST detection (the most complex case, $L = N_t$ )	38
Figure 3.4 Extension of the proposed algorithm	39
Figure 3.5 Simplified Multiplication Complexities of $H^H H$	41
Figure 4.1 Computation time comparison of the existing detection methods and the proposed methods ( $N_t = 4$ $N_r = 4$ )	47
Figure 4.2 Computation time comparison of the existing detection methods and the proposed methods ( $N_t = 4$ $N_r = 5$ )	47
Figure 4.3 Computation time comparison of the existing detection methods and the proposed methods ( $N_t = 4$ $N_r = 6$ )	48
Figure 4.4 BER performance versus SNR of various detection techniques (2x2), office environment	50
Figure 4.5 BER performance versus SNR of various detection techniques (2x3), office environment	51
Figure 4.6 BER performance versus SNR of various detection techniques (2x4), office environment	51

Figure 4.7 BER performance versus SNR of various detection techniques (3x3), office environment	52
Figure 4.8 BER performance versus SNR of various detection techniques (3x4), office environment	52
Figure 4.9 BER performance versus SNR of various detection techniques (3x5), office environment	53
Figure 4.10 BER performance versus SNR of various detection techniques (4x4), office environment	53
Figure 4.11 BER performance versus SNR of various detection techniques (4x5), office environment	54
Figure 4.12 BER performance versus SNR of various detection techniques (4x6), office environment	54
Figure 4.13 BER performance versus SNR of our various detection techniques and V-BLAST (4x4), office environment	55
Figure 4.14 BER performance versus SNR of our various detection techniques and V-BLAST (4x5), office environment	55
Figure 4.15 BER performance versus SNR of the proposed detection techniques and V-BLAST (4x6), office environment	56
Figure 4.16 BER performance versus SNR of various detection techniques (2x2), large hall environment	57
Figure 4.17 BER performance versus SNR of various detection techniques (2x3), large hall environment	57
Figure 4.18 BER performance versus SNR of various detection techniques (2x4), large hall environment	58
Figure 4.19 BER performance versus SNR of various detection techniques (3x3), large hall environment	58
Figure 4.20 BER performance versus SNR of various detection techniques (3x4), large hall environment	59
Figure 4.21 BER performance versus SNR of various detection techniques (3x5), large hall environment	59
Figure 4.22 BER performance versus SNR of various detection techniques (4x4), large hall environment	60
Figure 4.23 BER performance versus SNR of various detection techniques (4x5), large hall environment	60
Figure 4.24 BER performance versus SNR of various detection techniques (4x6), large hall environment	61
Figure 4.25 BER performance versus SNR of our various detection techniques and V-BLAST (4x4), large hall environment	61

Figure 4.26 BER performance versus SNR of our various detection techniques and V-BLAST (4x5), large hall environment	62
Figure 4.27 BER performance versus SNR of our various detection techniques and V-BLAST (4x6), large hall environment	62






# Chapter 1

## Introduction

### 1.1 Background



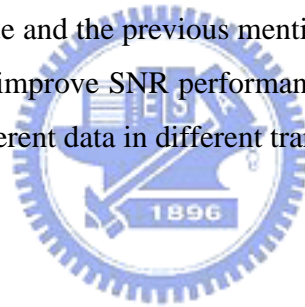
The fast growth of telecommunication service subscribers, the Internet, and the personal computing devices are witnessed in the recent decade and expected to continuous in the future. For wireless multimedia and data services we need robust, high-bit-rate and wide-area wireless networks. Hence, future wireless personal communication systems are expected to provide high performance transmission over hostile mobile environments regardless of mobility or location, although there are still technical problems to be solved for this objective [1]. When realizing broadband wireless systems, those severe effects of frequency-selective fading are difficult to resolve [2]. Traditionally, more bandwidth is required for higher data-rate transmission. However it is often impractical or sometimes very expensive to increase bandwidth. OFDM technique get lot of attraction in wireless transmission in recent years for advantages in mitigating the detrimental effects of frequency-selective fading [3,4,5].

Recent information theory on multiple input multiple output (MIMO) technology reveals that multipath wireless channels facilitate increase of spectral efficiency, provided that those multipath are sufficiently rich [6,7,8]. In such cases, the channel between each transmit and receive antenna pair is flat and uncorrelated. Space Division Multiplexing

(SDM) is a technique that can provide a significant improvement in capacity and bit error rate (BER) performance. Basically, different parallel data streams are transmitted, at the same time and on the same frequency, using an antenna array. When utilizing multiple antennas at the receiver as well, these data streams, mixed-up by the wireless channel, can be recovered by SDM techniques such as Vertical – Bell Laboratories Layered Space-Time (V-BLAST) [9] .

These algorithms require flat-fading channel information between each transmit and receive antenna pair. However, most practical channels are frequency-selective fading so that performances will be degraded. In OFDM systems frequency-selective fading become flat-fading in each subcarrier and is effective when combined with SDM techniques [10, 13].

Currently, plenty of researches are about applying transmitter and receiver diversity [14, 15] and space-time codes [16] to multicarrier techniques. The difference between the combined technique and the previous mentioned combined SDM and OFDM technique is that the latter can improve SNR performances as well as data rates, because it transmits simultaneously different data in different transmit antennas.



## 1.2 Motivations

In this thesis, we focus on telecommunication systems with rich scattering channels where SDM techniques have best performance. In addition, OFDM systems are studied, because it helps to turn the frequency-selective fading into flat-fading conditions. It is known that for each OFDM subcarrier, transmitted signals experience flat-fading channels. It conforms to the assumed conditions when using ZF and V-BLAST techniques.

In order to get better performance than V-BLAST, we propose a hybrid ML detection and V-BLAST detection, and reduce a good deal of complexities required by ML detection. To get knowledge on computational complexities and BER performances of the proposed algorithms, 802.11n systems with MIMO conditions are simulated. To

verify performances, we analyze and simulate, the proposed designs and some existing designs, with respect to BER and complexity.

### **1.3 Organization of the Thesis**

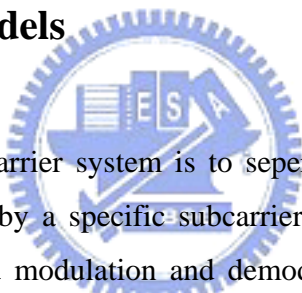
First, fundamentals of both OFDM and MIMO are studied in Chapter 2, and so are the techniques based on V-BLAST data detection. Besides, MIMO OFDM systems are also described in Chapter 2, followed by discussion of some existing enhanced algorithms for data detection. Chapter 3 introduces the proposed new enhanced MIMO OFDM data detection algorithms based on some major existing algorithms and the devised new idea, while Chapter 4 includes simulations. Simulations are performed according to EWC 802.11n specifications. Finally, we conclude with some remarks of the work in Chapter 5.



# Chapter 2

## OFDM and MIMO Fundamentals

### 2.1 OFDM System Models



The principle of multicarrier system is to separate the data stream into several parallel ones, each modulated by a specific subcarrier and discrete Fourier Transform (DFT) is used in the baseband modulation and demodulation. Through this approach, only a pair of oscillator (for I-part and Q-part) is needed instead of multiple oscillators to modulate different signals at different carriers.

When signals pass through a time-dispersive channel, inter-symbol interference (ISI) and inter-carrier interference (ICI) usually occur in the receiver and cyclic prefix (CP) is introduced to combat ISI and ICI. Cyclic prefix, shown in Figure 2.1, is a copy of the tail part of a symbol, which is inserted in between the symbol to be transmitted and its preceding symbol. As long as the cyclic prefix length is longer than its experiencing time-dispersive channel length, ISI can be avoided. At the same time, the cyclic prefix along with its symbol makes a periodic signal and maintains the properties of circular convolution and subcarrier orthogonality that prevents the ICI effect.



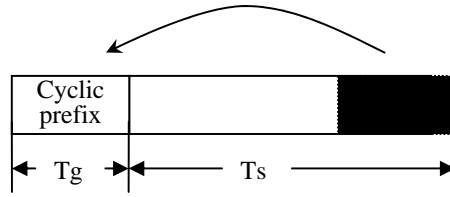


**Figure 2.1** Cyclic prefix of an OFDM symbol [18]

### 2.1.1 Continuous-Time Model

In this chapter, a continuous-time model is used to introduce the whole OFDM baseband system including the transmitter and receiver. In the transmitter, the transmitted data is split into multiple subchannels with overlapping frequency bands.

The spectrum of OFDM signal is shown in Figure 2.2. It is clear that the spectrum of each subchannel is spreading to all the others, but is zero at all the other subcarrier frequencies, because of the sinc function property, which is the key feature of the orthogonality.

Assume the given channel is quasi-static, i.e., constant during the transmission of an OFDM symbol and variable symbol wise, where the quasi-static impulse response is  $h(n,m)$ ,  $n$  is the time index and  $m$  is the channel path delay. The received signal  $y(t)$  can be expressed as

$$y(t) = h(n,m) * x(t) + n(t) \quad (2.1)$$

where  $x(t)$  is the transmitted data and  $n(t)$  is the additive white Gaussian noise.

Figure 2.3 (a) shows a typical continuous-time OFDM baseband modulator, in which the transmitted data is split into multiple parallel streams which are modulated by different subcarriers and then transmitted simultaneously. At the receiver, the received signal is demodulated simultaneously by multiple matched filters and then the data on each subchannel is obtained by sampling the outputs of matched filters, as shown in Figure 2.3 (b).

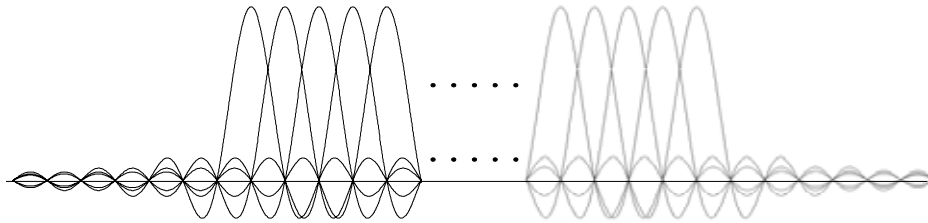


**Figure 2.2** Spectrum of an OFDM signal [18]

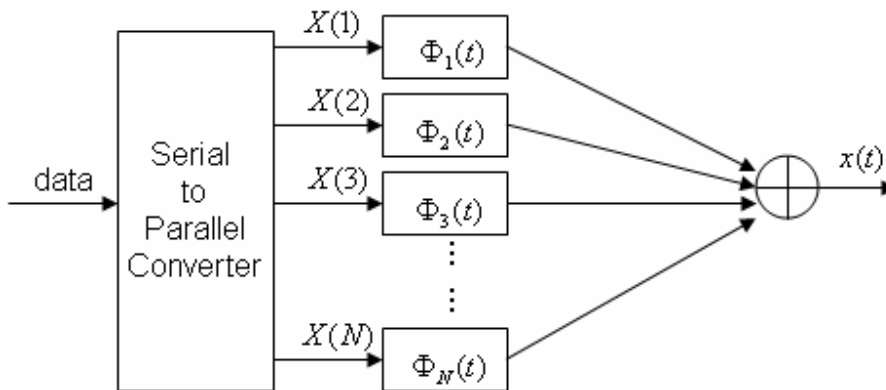


**Figure 2.3 (a)** Continuous-time OFDM baseband modulator [18]

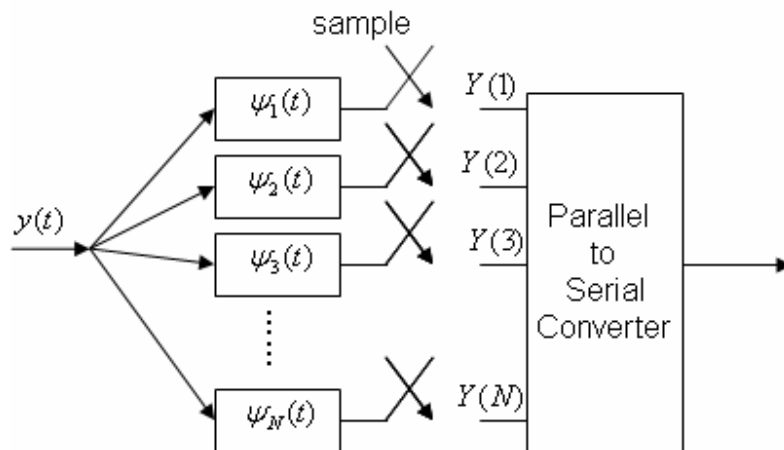


**Figure 2.3 (b)** Continuous-time OFDM baseband demodulator [18]

## 2.1.2 Discrete-Time Model

As mentioned previously, to simultaneously transmit multiple data, the transmitter must modulate data with multiple subcarriers and the receiver must demodulate with multiple matched filters. In fact, the modulation and demodulation can be implemented efficiently by using digital IDFT/DFT operations, because they can be respectively represented as

$$x(i) = \sum_{k=0}^{N-1} X(k)e^{j\frac{2\pi}{N}ki} = \sum_{k=0}^{N-1} X(k)\phi_k(i) \quad (2.2)$$

$$Y(k) = \sum_{i=0}^{N-1} y(i)e^{-j\frac{2\pi}{N}ki} = \sum_{i=0}^{N-1} y(i)\psi_k(i) \quad (2.3)$$

which are the same as IDFT operation of the transmitted data  $X(k)$  and DFT operation of the received data  $y(i)$ , respectively.

Figure 2.4 shows the discrete-time baseband OFDM model. The IDFT transforms the frequency-domain data into time-domain data which is delivered over the air and passed through a multi-path channel, denoted as  $h(n,m)$ . At the receiver, to recover the signal in frequency domain, DFT is adopted in the demodulator as a matched filter. Then the frequency-domain signal of each subchannel is obtained from its DFT output.

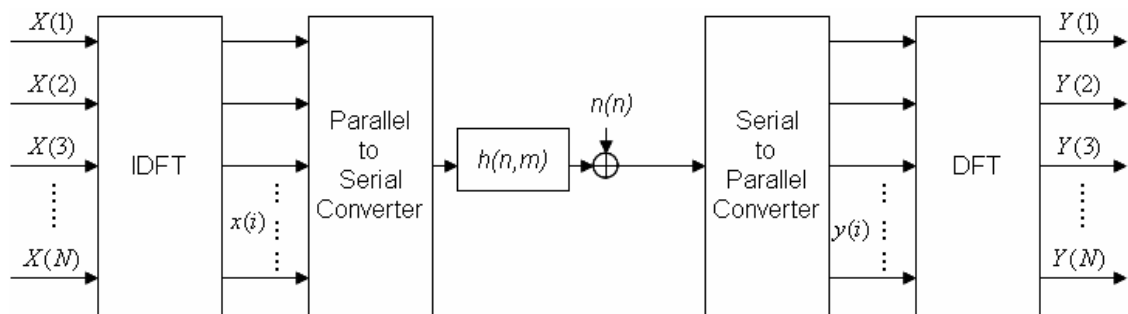


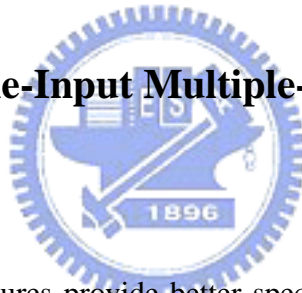
**Figure 2.4** Discrete-time OFDM system model [18]

### 2.1.3 Effect of Cyclic Prefix

Because of multipath channels, orthogonality as shown in Figure 2.2 will be destroyed by ISI and ICI. However, as long as the cyclic prefix length is longer than that of  $h(n,m)$ , ISI effect can be avoided. It is known that circular convolution in time domain results in multiplication in frequency domain when the channel is stationary so that the received signal  $y(k)$  in frequency domain is the product of transmitted data  $x(k)$  and subcarrier channel response  $H(k)$ . Thus, the orthogonality is maintained (if  $h(n,m)$  is fixed within the symbol length) and data can be easily recovered by one-tap channel equalizer, i.e., dividing  $y(k)$  by the corresponding  $H(k)$ .

$$y(k) = H(k) \times x(k) + n(k) \quad (2.4)$$

## 2.2 Concept of Multiple-Input Multiple-Output (MIMO) Systems



MIMO system architectures provide better spectral efficiency than conventional systems, because of the benefit of multiple antenna or space diversity both at the transmitter and receiver.

MIMO systems provide the ability to turn multipath propagation, which is traditionally a drawback of wireless transmission, into a benefit. Since MIMO systems effectively take advantage of random fading and multipath delay spread, the signals transmitted from each transmit antenna appear highly uncorrelated at each receive antenna and the signals travel through different spatial channels. Then the receiver can exploit these different spatial channels and separate the signals transmitted from different antennas at the same frequency band simultaneously.

## 2.2.1 MIMO System Model

MIMO is a promising technology suited for high-speed broadband wireless communications. Through space division multiplexing, MIMO technology can transmit multiple data streams in independent parallel spatial channels, thereby increasing total system transmission rate.

MIMO systems can be easily defined. Considering an arbitrary wireless communication system, a link is considered for which the transmitter is equipped with  $N_t$  transmit antennas and the receiver is equipped with  $N_r$  receive antennas. Such a setup is illustrated in Figure. 2.5. Consider this system some important assumptions are made first:

1. Channels are constant during the transmission of a packet. It means the communication is carried out in packets that are of shorter time-span than the coherence time of the channels.

2. Channels are memoryless. It means that an independent channel realization is drawn for each use of the channels.

3. The channel is flat fading. It means that constant fading over the bandwidth is desired in the case of narrowband transmissions. It also indicates that the channel gains can be represented by complex numbers.

4. The received signal is corrupted by AWGN only.

With these assumptions, it is common to represent the input/output relations of a narrowband, single-user MIMO link by the complex baseband vector notation

$$y = Hx + n \quad (2.5)$$

where  $x$  is the  $N_t \times 1$  transmit vector,  $y$  is the  $N_r \times 1$  receive vector,  $H$  is the  $N_r \times N_t$  channel matrix, and  $n$  is the  $N_r \times 1$  additive white Gaussian noise (AWGN) vector at some instant in time. All the coefficients  $h_{ij}$  comprise the channel matrix  $H$  and represent the complex gain of the channel between the  $j$ th transmit antenna and the  $i$ th receive antenna. The channel matrix can be written as

$$H = \begin{pmatrix} h_{11} & h_{12} & \cdots & h_{1N_t} \\ h_{21} & h_{22} & \cdots & h_{2N_t} \\ \vdots & \vdots & \ddots & \vdots \\ h_{N_r,1} & h_{N_r,2} & \cdots & h_{N_r,N_t} \end{pmatrix} \quad (2.6)$$

$$h_{ij} = \alpha_{ij} + \beta_{ij}j = |h_{ij}| \cdot e^{j\phi_{ij}} \quad (2.7)$$

Coefficients  $\{h_{ij}\}$  reflect unknown channel properties of the medium, usually Rayleigh distributed in a rich scattering environment without line-of-sight (LOS) path. If  $\alpha_{ij}$  and  $\beta_{ij}$  are independent and Gaussian distributed random variables, then  $|h_{ij}|$  is a Rayleigh distributed random variable. Actually, coefficients  $\{h_{ij}\}$  are likely to be subject to varying degrees of fading and change over time. Therefore, determination of the channel matrix is an important and necessary aspect of MIMO techniques. If all these coefficients are known, there will be sufficient information for the receiver to eliminate interference from other transmitters operating at the same frequency band.

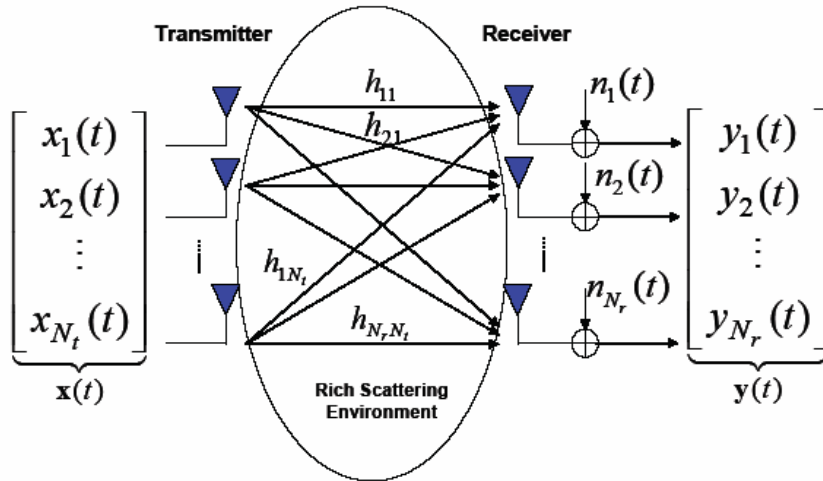


**Figure 2.5** Wireless MIMO transmission model [17]

Although the introduced MIMO transmission requires flat-fading channels, and it is limited to applications with narrowband transmissions, in real broadband transmission systems, channel conditions are often frequency-selective fading. A technique alleviating severe effect of frequency-selective fading is demanded. OFDM technique is a good solution for this purpose in wireless transmission owing to its advantages [3,4,5].

## 2.2.2 MIMO-OFDM Architecture

According to Section 2.1, OFDM technique turns frequency-selective fading channel into several flat-fading subchannels, and it solves the major problem in wideband transmission systems. Boubaker et. al [10] proposed V-BLAST technique to detect transmitted signals on each subcarrier of a MIMO OFDM system. MIMO OFDM transceiver and receiver architectures are shown in Figures 2.6 and 2.7, respectively.

Subchannels are orthogonal to each other in OFDM systems. Hence, in a single-input-single-output (SISO) OFDM systems, the received signals are product of channel response and transmitted signal, as shown in equation 2.4. In MIMO systems, signals transmitted from different antennas on a subcarrier simultaneously interfere each other, but signals at different subcarriers are independent. At each receiver antenna, a linear combination of the transmitted signal and channel response on each subcarrier is observed. That corresponds to assumptions of MIMO systems. On each subchannel, a space division multiplexing (SDM) like V-BLAST is applied. That is, the task is to recover  $x$  from the received signal  $y$  and channel state information (CSI)  $H$  on each subcarrier.

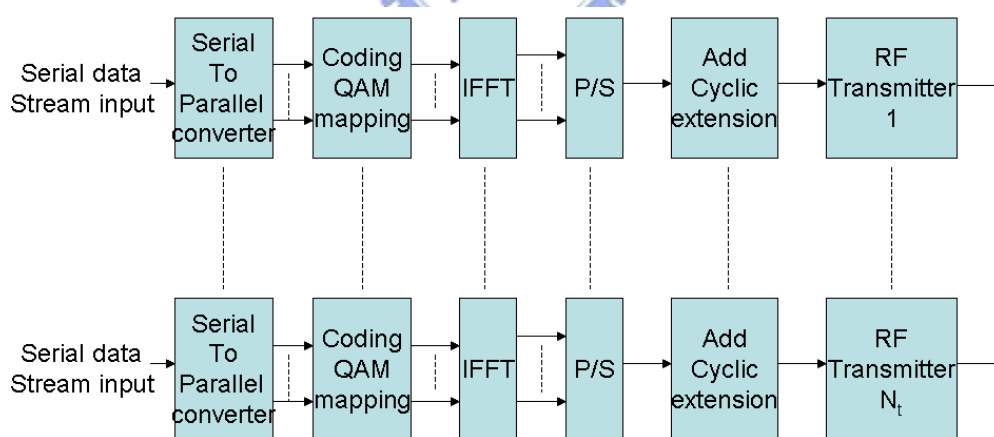


**Figure 2.6** Transmitter architecture of a MIMO OFDM system [10]

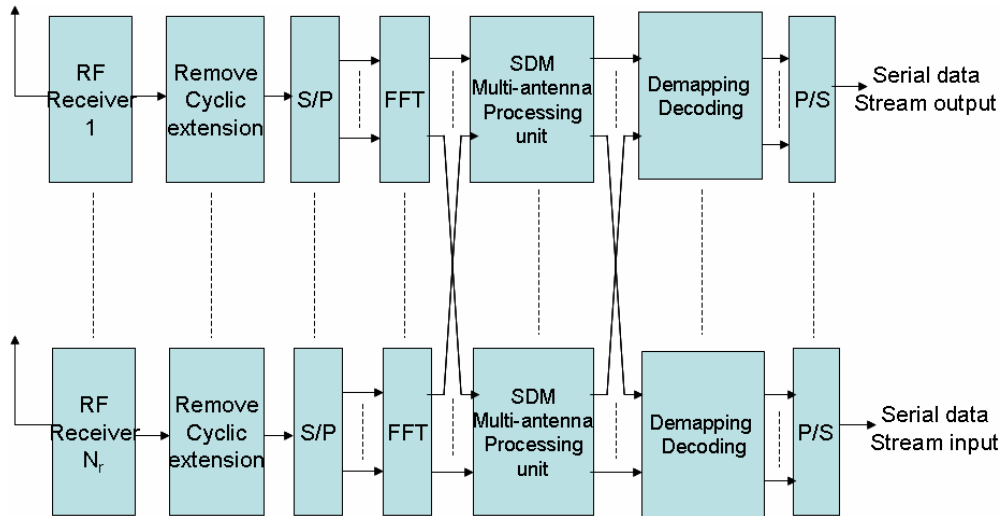


**Figure 2.7** Receiver architecture of a MIMO OFDM system [10]

### 2.2.3 An example MIMO OFDM System EWC 802.11n

EWC 802.11n standard utilize both MIMO and OFDM techniques for high throughput transmission of wireless LAN. EWC 802.11n proposal [11] emphasizes backward compatibility with existing installed base, building on experience with interoperability in 802.11g and previous 802.11 amendments which are mainly designed for indoor wireless internet applications. Hence, we review the physical layer of wireless LAN 802.11a [12] system which is based on OFDM technology. The main system parameters of IEEE 802.11n Wireless LAN standard are listed in Table 2.1.

In 802.11n standard, a frame is composed of three fields. Table 2.1 shows the packet format which facilitates synchronization and channel estimation of the receiver. In the preamble field, the preambles are composed of ten repeated short symbols and two repeated long symbols. The total duration of short symbols is  $8 \mu s$  and so is that of long symbols. Since the SIGNAL field contains the most important information of a packet, such as frame length and modulation, synchronization and channel estimation must be finished before decoding of the SIGNAL field.



To examine validity of proposed algorithms in latter chapters, EWC 802.11n standard, is adopted for simulation.

**Table 2.1** Parameters and specifications of EWC 802.11n systems [11]

Parameter	Value in legacy 20MHz channel	Value in HT 20MHz channel	Value in 40MHz channel	
$N_{SD}$ : Number of data subcarriers	48	52	108	48 <sup>1</sup>
$N_{SP}$ : Number of pilot subcarriers	4	4	6	8 <sup>1</sup>
$N_{ST}$ : Total Number of subcarriers	52	56	114	
$N_{SR}$ : Number of subcarriers occupying half of the overall BW	26	28	58	
$\Delta_f$ : subcarrier frequency spacing	312.5kHz (20MHz/64)	312.5kHz	312.5kHz (40MHz/128)	
$T_{FFT}$ : IFFT/FFT period	3.2 $\mu$ sec	3.2 $\mu$ sec	3.2 $\mu$ sec	
$T_{GI}$ : Guard Interval length	0.8 $\mu$ sec = $T_{FFT}/4$	0.8 $\mu$ sec	0.8 $\mu$ sec	
$T_{GI2}$ : Double GI	1.6 $\mu$ sec	1.6 $\mu$ sec	1.6 $\mu$ sec	
$T_{GIS}$ : Short Guard Interval length	0.4 $\mu$ sec = $T_{FFT}/8$	0.4 $\mu$ sec	0.4 $\mu$ sec	
$T_{L-STF}$ : Legacy Short training sequence length	8 $\mu$ sec = $10 \times T_{FFT}/4$	8 $\mu$ sec	8 $\mu$ sec	
$T_{L-LTF}$ : Legacy Long training sequence length	8 $\mu$ sec = $2 \times T_{FFT} + T_{GI2}$	8 $\mu$ sec	8 $\mu$ sec	
$T_{SYM}$ : Symbol Interval	4 $\mu$ sec = $T_{FFT} + T_{GI}$	4 $\mu$ sec	4 $\mu$ sec	
$T_{SYMS}$ : Short GI Symbol Interval	3.6 $\mu$ sec = $T_{FFT} + T_{GIS}$	3.6 $\mu$ sec	3.6 $\mu$ sec	
$T_{L-SIG}$	4 $\mu$ sec = $T_{SYM}$	4 $\mu$ sec	4 $\mu$ sec	

In 802.11n, a PLCP (PHY Layer Convergence Protocol) frame shall have one of the following three formats, the field parameters are define below:

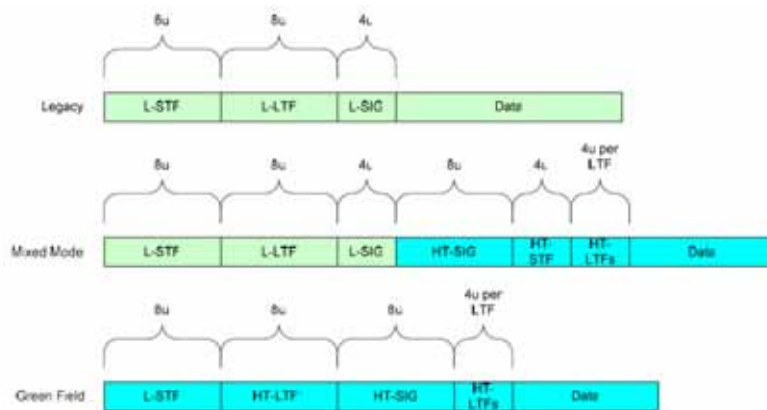


**Figure 2.8** PLCP frame format of EWC 802.11n standard [12]

L-STF: Legacy Short Training Field.

L-LTF: Legacy Long Training Field.

L-SIG: Legacy Signal Field.

HT-SIG: High Throughput Signal Field.

HT-STF: High Throughput Short Training Field.

HT-LTF1: First High Throughput Long Training Field.

HT-LTF's: Additional High Throughput Long Training Fields.

Data: The data field includes the PSDU (PHY Sub-Layer Data Unit).

The PHY will operate in one of 3 modes:

-Legacy mode: in this mode the packets are transmitted with 802.11a/g format.

-Mixed mode: in this mode packets are transmitted with a preamble compatible with the legacy 802.11a/g – the legacy Short Training Field (STF), the legacy Long Training Field (LTF) and the legacy signal field are transmitted so they can be decoded by legacy 802.11a/g devices. The rest of the packet has a new format. In this mode the receiver shall be able to decode both the Mixed Mode packets and legacy packets.

-Green Field: in this mode high throughput packets are transmitted without a legacy compatible part. This mode is optional. In this mode the receiver shall be able to decode both Green Field mode packets and legacy format packets.

We can choose an appropriate mode for the compatibility with former standards.

For the purpose of compatibility with 802.11 legacy devices, the legacy part of the preamble format in EWC proposal is the same as that in 802.11a. If the legacy preambles are transmitted from multiple antennas, the mapping of this single spatial stream to multiple antennas has to be done such that beamforming in far-field is mitigated. One method for achieving this is to use a cyclical-delay-diversity (CDD) mapping. The cyclical delay is adopted in EWC proposal, whose format is used for simulation. Figure 2.9 shows the cyclical delay format in EWC. The maximum number of the spatial data streams is four. STRN stands for the short training sequence. LTRN represents the long training symbol. GI2 is the guard interval of the long training symbol.

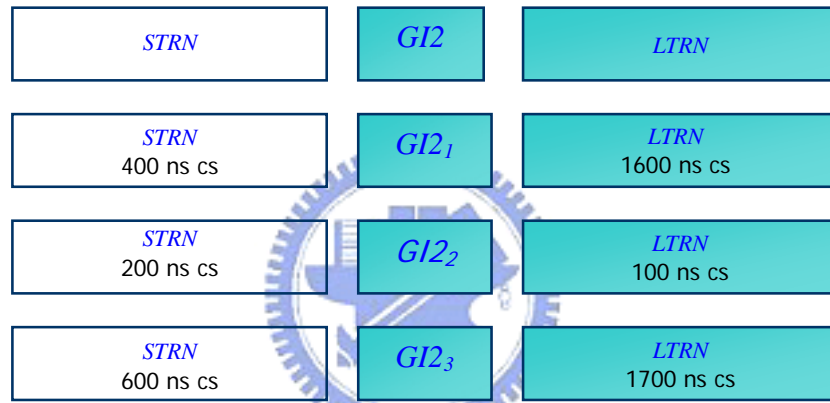


**Figure 2.9** Cyclical delay format of the preamble in EWC 802.11n standard [11]

## 2.3 Signal Detection Algorithms for MIMO Systems

Signal detection here means a process that try to recover the transmitted signals at receivers. As shown in equation 2.5, the task is to detect the transmitted vector  $x$  based on received vector  $y$  and channel state information (CSI)  $H$ .

In this section zero-forcing (ZF) criterion is considered due to consideration of low complexity. Zero-forcing techniques receive an input vector  $y$  and send it to a filter bank which eliminates the mutual interference without caring about noise.

### 2.3.1 Maximum-Likelihood (ML) Detection

Since modern transmission systems are digital, each element of transmitted vector  $x$  is chosen from a finite set, which is denoted as  $A$ , such as BPSK, QPSK and 16-QAM. Hence, a transmitted signal  $x$  belongs to the multiplicative set  $A^{N_t}$ . The optimum maximum-likelihood (ML) detector searches over the whole set of transmit signals  $x \in A^{N_t}$ , and decides in favor of the transmit signal  $x_{ML}$  that minimizes the Euclidian distance to the receive vector  $y$ , i.e.

$$x_{ML} = \arg_{x \in A^{N_t}} \min \|y - Hx\|^2 \quad (2.8)$$

The computational effort is of order  $M^{N_t}$ , where  $M$  denotes the size of finite set  $A$ . When using high modulation scheme or a large number transmitting antennas, ML detection is impractical.

### 2.3.2 V-BLAST Detection Method

Although ML detection reaches optimal performance, it is not feasible for large numbers of transmit antennas or high modulation schemes. In the sequel, some suboptimal algorithms are investigated. The target is to find algorithms that have performance near ML and low complexities.

Vertical – Bell Laboratories Layered Space-Time (V-BLAST) [9] is proposed to improve performance of the linear detection method by utilizing successive interference cancellation based on zero-forcing criterion. It suggests that transmitted signals are detected sequentially rather than in parallel. In each detection step, the signal which yields the smallest estimation error is linearly detected. It is shown in [9] that row  $g_{ZF}$ , the row with the minimum norm in  $G_{ZF}$  ( $G_{ZF} = H^+ = (H^H H)^{-1} H^H$ ), has the largest signal-to-noise ratio (SNR) and yields the smallest estimation error, because it causes minimum noise enhancement.

$$\hat{x}_i = g_{ZF}^i y = g_{ZF}^i (Hx + n) = x_i + \eta_i \quad (2.9)$$

where  $i$  is the order index a signal is detected.

$\hat{x}_i$  is quantized to obtain estimate of  $x_i$ , and the interference of this signal is removed by subtracting it from the received signal  $y$ , so is the  $i$ -th column of the channel matrix is nulled. Nulling and canceling process are repeated until all signals are detected, as summarized in the following algorithm steps:

Begin

$$H^1 = H \quad (2.10.a)$$

$$y_1 = y \quad (2.10.b)$$

$$\text{for } (i=1; i \leq N_t; i++) \quad (2.10.c)$$

$$G_{ZF}^i = (H^i)^+ \quad (2.10.d)$$

$$k_i = \arg_i \min \|G_{ZF}^i\| \quad (2.10.e)$$

$$g_{ZF}^i = (G_{ZF}^i)_{k_i} \quad (2.10.f)$$

$$\hat{x}_i = g_{ZF}^i y \quad (2.10.g)$$

$$x_{k_i} = \text{quantize}(\hat{x}_i) \quad (2.10.h)$$

$$y_{i+1} = y_i - x_{k_i} H_{k_i} \quad (2.10.i)$$

$$H^{i+1} = H_{k_i}^i \quad (2.10.j)$$

end

where  $(G)_i$  means  $i$ -th row of  $G$ ,  $H_{k_i}$  means  $k_i$ -th column of  $H$ , and  $H_{k_i}^i$  means the resulting  $H$  matrix after nulling the  $k_i$ -th column of  $H^i$ .

The main computational bottleneck in the iterative process is the computation of pseudo inverses for  $N_t$  matrices. For saving computation, channel response is assumed constant within a packet, as assumption 1 suggests. The optimal detection order and each nulling vector  $g_{ZF}$  are validly used to detect received signals in the whole packet, because they share the same channel matrix. That is, pseudo inverse of the channel is not updated.

### 2.3.3 Detection Methods based on V-BLAST

We will introduce four different algorithms based on V-BLAST technique. The first algorithm reduces the numbers of pseudo-inverse operations. The second algorithms can increase performance by reducing negative side effects. The first and second algorithms consider trade-off in the iteration process of V-BLAST techniques. The third algorithm is MMSE-VBLAST that includes the noise term in the design of the linear filter matrix  $G$ . The fourth algorithm is based on parallel symbol cancellation (PSC) instead of serial symbol cancellation (SSC). It focuses on detecting signals at the same time.

#### 2.3.3.1 Simplified V-BLAST Detection

On each subcarriers of a MIMO OFDM system, a V-BLAST detector is used, because we can formulate the detection problem of each subchannel by equation 2.5. Hence for practical OFDM systems, there will involve a lot of V-BLAST detectors. Fortunately, channel responses of successive subcarriers are often similar. Some simplified algorithms [13,20] are proposed based on this observation.

[13] assumed that successive subcarriers have the same channel response so that calculated vectors of a subcarrier are applied to detect signals of nearby subcarriers. We can call this algorithm a simplified 0th-order algorithm.

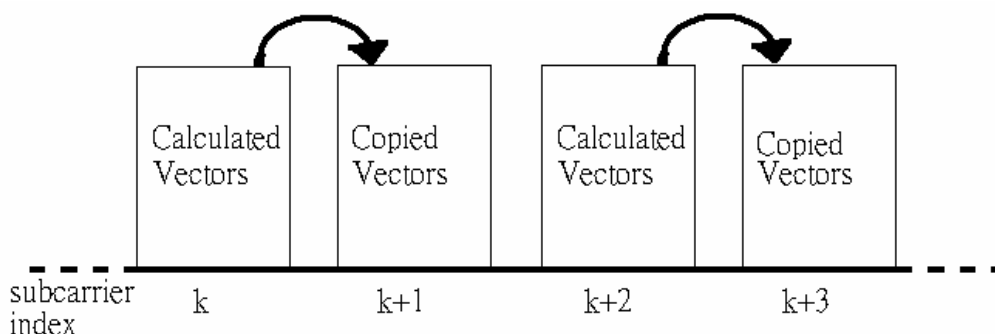


**Figure 2.10** The 0th-order simplified V-BLAST detection algorithm in [13]

The subcarrier which is decoded by approximation is assumed to have the same decode order as that of the subcarrier which provides the pseudo inverse. At each step of V-BLAST detection, a column of channel matrix is set to zero in order to ignore the effect of the corresponding transmitting antenna. If the pseudo inverse is used to estimate inverse of adjacent subcarriers, the subcarriers have to recognize the nulled columns, which stand for the detected signals. In other words, the optimal decoding order is assumed unchanged.

Under this assumption, there are some opportunities for further simplification. The simplified algorithm has identical performance but with lower complexities. Owing to unchanged decoding order it merely needs a row of the approximated pseudo inverse which represents the transmitted signal to be detected, rather than the whole pseudoinverse, as shown below.

$$\left[ H(k+1, p)^+ \right]_j \approx \left[ H(k, p)^+ + H(k, p)^+ (H(k, p) - H(k+1, p)) H(k, p)^+ \right]_j \quad (2.11)$$

where  $[ ]_j$  denotes the  $j$ -th row, and  $p$  is a small enough positive integer.

$$\left[ H(k+1, p)^+ \right]_j \approx \left[ H(k, p)^+ \right]_j + \left[ H(k, p)^+ (H(k, p) - H(k+1, p)) H(k, p)^+ \right]_j \quad (2.12)$$

then

$$\left[ H(k+1, p)^+ \right]_j \approx \left[ H(k, p)^+ \right]_j (1 + (H(k, p) - H(k+1, p)) H(k, p)^+) \quad (2.13)$$

As a result, computation complexity is reduced, but performance is not noticeably degraded. This simplified algorithm can be called a 1st-order simplified algorithm. Its algorithm steps are summarized below.

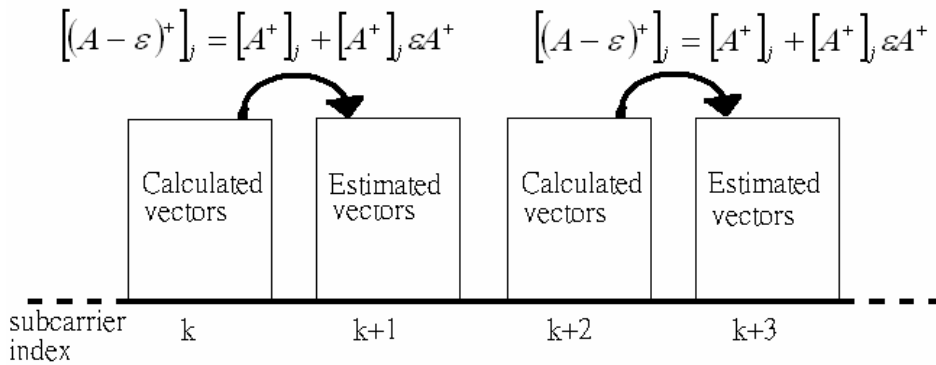


**Figure 2.11** The simplified V-BLAST detection algorithm in [18]

```

Begin
for ( $i=1$  ;  $i \leq$  subcarrier number ;  $i+=2$ ) (2.14.a)
    calculate weight vectors  $g_{ZF}^i$  according to equation (2.10) (2.14.b)
    if successive subcarriers share a channel response [13] (2.14.c)
         $g_{ZF}^{i+1} = g_{ZF}^i$  (2.14.d)
    else // (2.14.e)
        calculate weight vectors  $g_{ZF}^{i+1}$  according to equation (2.13) (2.14.f)
    end (2.14.g)
end (2.14.k)

```

### 2.3.3.2 Enhanced V-BLAST Detection

Since V-BLAST's performance is worse than ML detection, improved detection methods [19,21,22] based on V-BLAST technique are proposed to get better performance than the conventional V-BLAST technique.

#### 2.3.3.2.1 Two Iterative V-BLAST Detection Algorithms

##### Shen's Approach [19]:

An iterative V-BLAST detection algorithm improving the performance over error propagation is proposed [19]. In the algorithm, low-diversity substreams are iteratively decoded by using decisions from high-diversity substreams. As such the performance is greatly improved over the conventional one. Another advantage of this algorithm is that it is practical to make a trade-off between performance and complexity. The steps of the algorithm is listed below. Table 2.2 also illustrates the algorithm.

*initialization:*

*Step 1:*

*detect  $\hat{x}_1, \hat{x}_2, \dots, \hat{x}_{N_t}$  by V-BLAST*



Step 2:

for  $i=1$  to  $N_t-1$

subtract signals from substreams 1 to  $i$  ( $\hat{x}_1, \hat{x}_2, \dots, \hat{x}_i$ ) as

$$\hat{y} = y - \sum_{j=1}^i H_j \hat{x}_j \quad (2.15)$$

apply the V-BLAST detection to generate  $\hat{x}_{N_t-i}$

end

**Table 2.2** Change of diversity degree in each V-BLAST's loop [19]

No. of Loop	Detection order	Detected Symbol
Initialization	$\hat{x}_1 \rightarrow \hat{x}_2 \dots \dots \rightarrow \hat{x}_{N_t}$	$\hat{x}_{N_t}$
Loop 1	$\hat{x}_{N_t} \rightarrow \hat{x}_1 \rightarrow \hat{x}_2 \dots \hat{x}_{N_t-1}$	$\hat{x}_{N_t-1}$
Loop 2	$\hat{x}_{N_t}, \hat{x}_{N_t-1} \rightarrow \hat{x}_1 \rightarrow \hat{x}_2 \dots \hat{x}_{N_t-2}$	$\hat{x}_{N_t-2}$
:		:
:		:
Loop $N_t$	$\hat{x}_{N_t}, \hat{x}_{N_t-1}, \dots, \hat{x}_2 \rightarrow \hat{x}_1$	$\hat{x}_1$

### Li's Approach [21]:

In this approach proposed iterative method [21] to suppress error propagation and improve the performance in an uncoded case. From simulation results, this method exhibits considerable performance gains over the original V-BLAST detection algorithm and the iterative algorithm presented in [19]. At the same time, this method has a lower complexity compared with the iterative method in [19].

Since the detected symbol  $\hat{x}_{N_t}$  has a diversity order of  $N_r$ , the new-version symbols of  $\hat{x}_1 \dots \hat{x}_{N_t-1}^{new}$  are more accurate than the old version. Such an improvement is especially obvious for symbol  $\hat{x}_1$ , because the new-version  $\hat{x}_1$  has the diversity order of  $N_r$  while the old one only has the diversity order of 1. By using such an approach, closed-loop iteration architecture for V-BLAST detector can be constructed. In detail, if the new-version  $\hat{x}_1$  is different from the old one, repeat above procedure. Otherwise, terminate the procedure and the symbol of  $\hat{x}_{N_t}$  as well as the present new-version  $\hat{x}_1^{new} \dots \hat{x}_{N_t-1}^{new}$  will be the final output of the detector. The method's steps are summarized

below.  $\tilde{H}_{i-1}$  means the resulting  $H$  matrix after nulling the  $i$ -1th column of  $H$ .

*Step 1:*

*Initialize the iteration number as IterNum=0.*

*Step 2:*

*Perform the optimal ordering and SIC using V-BLAST method and get the detected symbols  $\hat{x}_1^{old}, \hat{x}_2^{old} \dots \hat{x}_{N_t}$  (the optimal order is assumed to be 1,2,... $N_t$ )*

*Step 3:*

$$\tilde{H} = H$$

$$\tilde{y} = y; \hat{x}_{N_t}^{new} = \hat{x}_{N_t}$$

*for*  $i = N_t - 1$  *to* 1

$$\tilde{y} = \tilde{y} - \tilde{H}_{i-1} \hat{x}_{N_t-1}^{new}$$

$$\tilde{H} = \tilde{H}_{i-1};$$

$$\hat{x}_i = (\tilde{H}^+)_i \cdot \tilde{y}$$

$$\hat{x}_i = Q(\hat{x}_i)$$

*end*

$IterNum = IterNum + 1;$

Step 4:

If  $IterNum = MaxIterNum$  OR  $\hat{x}_1^{new} = \hat{x}_1^{old}$

goto step 5;

Else

$\hat{x}_1^{old} = \hat{x}_1^{new}$

goto step 4;

End

Step 5:

$\tilde{H} = H$

$\tilde{y} = y;$

for  $i = N_t - 2$  downto 1

$\tilde{y} = \tilde{y} - \tilde{H}_{i+1} \cdot \hat{x}_{i-1}^{old}$

$\tilde{H} = \tilde{H}_{i+1};$

$\hat{x}_i = (\tilde{H}^+)_i \cdot \tilde{y}$

$\hat{x}_i^{old} = Q(\hat{x}_i)$

End

$\hat{x}_0 = \hat{x}_0^{old};$

goto step 2

Step 6:

End of iteration and the final detected symbols are  $\hat{x}_1, \hat{x}_2, \dots, \hat{x}_{N_t}$

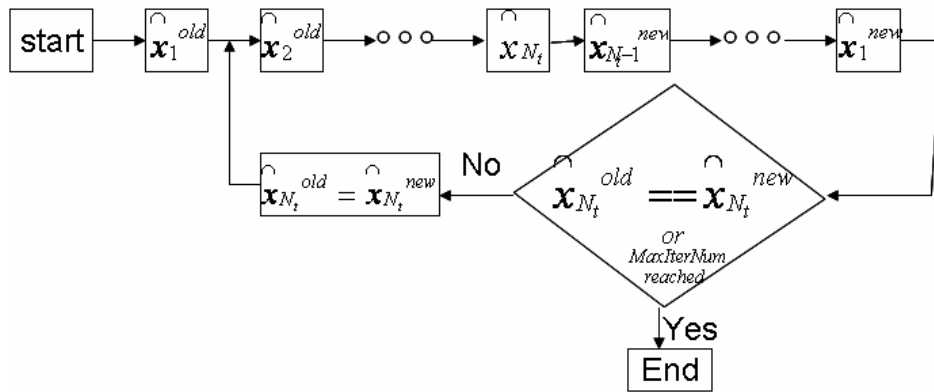


**Figure 2.12** Li's iterative V-BLAST detection algorithm [21]

Assumed that  $x_1 \dots x_{N_t-1}^{new}$  are detected in two iterations, Shen's approach requires more pseudoinverses than those of the Shen's approach. But their performances are the same [21]. Therefore, we will compare the second approach with the proposed methods in the latter chapters.

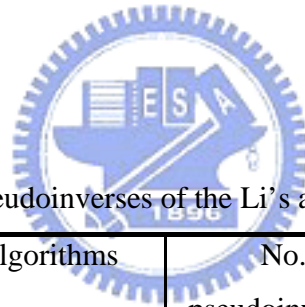


**Table 2.3** Number of pseudoinverses of the Li's and Shen's approaches [21]

Algorithms	No. pseudoinverses
Original V-BLAST	$N_t$
Shen's approach	$\frac{N_t(N_t + 1)}{2}$
Li's approach	$2N_t - 1$

### 2.3.3.2 Enhanced Zero-Forcing V-BLAST Detection

In their article [22], the authors concentrate on ZF decoding in V-BLAST technique and show that the ordering design in the algorithm has some negative side effects. Those effects reduce algorithm's performance. An improved ordering scheme is then proposed for ZF V-BLAST decoding.

Figure 2.11 [22] demonstrates the behavior of equation  $(\|\hat{n}_i\|^2)$  with a solid curve and the lower/upper bounds of

$$(d - \|\hat{n}_i\|)^2 \leq \|y_i - \hat{n}_i\|^2 \leq (d + \|\hat{n}_i\|)^2 \quad (2.16)$$

(when  $d = \sqrt{2}$ ,  $0 \leq \|\hat{n}_i\| \leq d$ ) in dotted lines. Divide equation (2.16) by  $\|\hat{n}_i\|^2 + K$ , one can get

$$\frac{(d - \|\hat{n}_i\|)^2}{\|\hat{n}_i\|^2 + K} \leq \frac{\|y_i - \hat{n}_i\|^2}{\|\hat{n}_i\|^2 + K} \leq \frac{(d + \|\hat{n}_i\|)^2}{\|\hat{n}_i\|^2 + K} \quad (2.17)$$

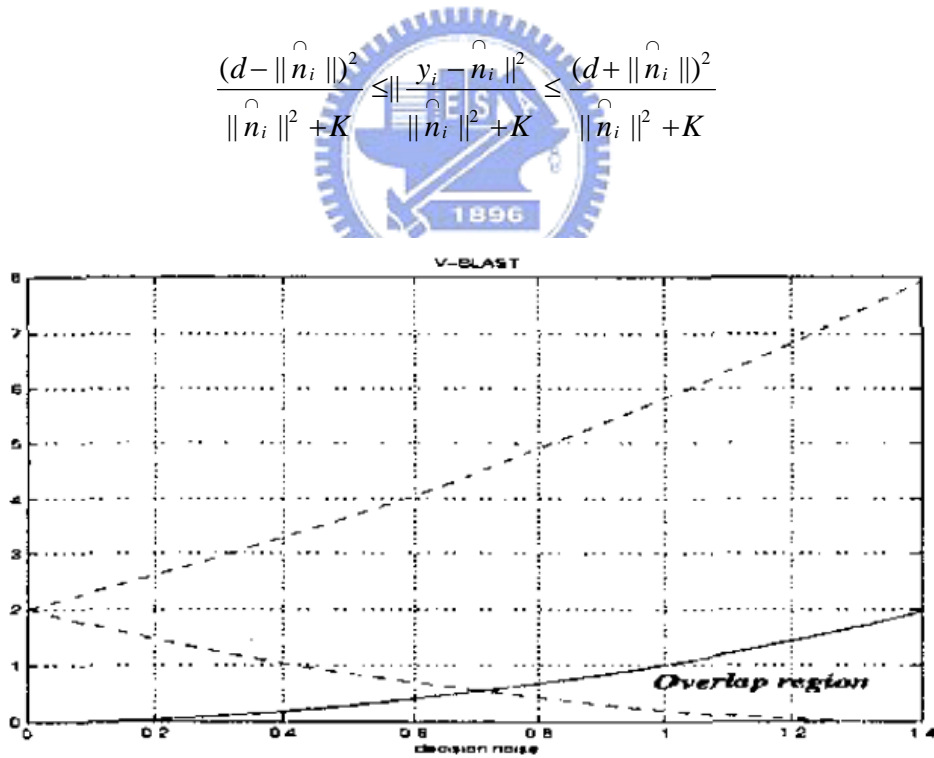


Figure 2.13 plot of equation (2.16) vs.  $\|\hat{n}\|$  [22]

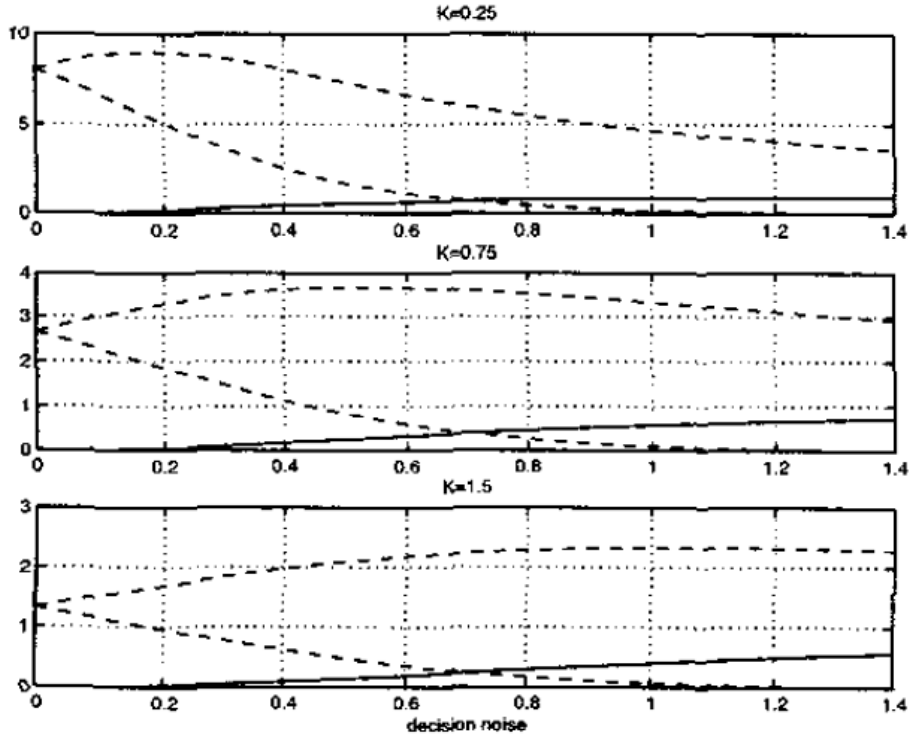
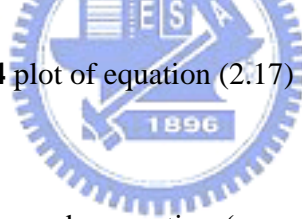


Figure 2.14 plot of equation (2.17) vs.  $\|\hat{n}\|$  [22]



Conventionally,  $k_i$  is chosen by equation ( $k_i = \arg \min_i \|G_{ZF}^i\|$ ). Different  $K$  will make different sizes of overlap regions. The smallest overlap region can be obtained in the figure. Therefore, better performance will be obtained by choosing the smallest overlap region. The overlapping region starts to occur when  $\|\hat{n}_i\|$  is relatively large. One can normalize the cost function by factor  $\|\hat{n}_i\|^2 + K$ . Therefore  $k_i$  is obtained by

$$k_i = \arg \min_i \frac{\|G_{ZF}^i\|}{\|\hat{n}_i\|^2 + K} \quad (2.18)$$

Simulation results [22] show that the new ranking will get better performance than conventional V-BLAST technique.

### 2.3.3.2.3 Joint ML and DFE Scheme for V-BLAST

In this approach [23], the authors present a detection algorithm, which combines ML and DFE schemes for V-BLAST method. It can improve V-BLAST method's performance by employing ML detection after V-BLAST detection. It makes a trade-off between complexity and performance, and shows that its performance is better than V-BLAST detection.

$$x_{ML} = \arg_{x \in A^{N_t}} \min \left\| \begin{bmatrix} y_1 \\ y_2 \\ \vdots \\ y_p \\ \vdots \\ y_{N_r} \end{bmatrix} - \begin{bmatrix} h_{11} & \bullet & h_{1p} & \bullet & h_{1N_t} \\ \bullet & & & & \bullet \\ \bullet & & & & \bullet \\ h_{p1} & & h_{pp} & & \bullet \\ \bullet & & & & \bullet \\ h_{N_r,1} & \bullet & h_{N_r,p} & \bullet & h_{N_r,N_t} \end{bmatrix} \begin{bmatrix} x_1 \\ \bullet \\ \bullet \\ x_p \\ \bullet \\ x_{N_t} \end{bmatrix} \right\|^2$$

**Figure 2.15** ML detection equation (number of transmitter antennas =  $N_t$ )

$$x_{ML} = \arg_{x \in A^{N_t}} \min \left\| \begin{bmatrix} y_1 \\ y_2 \\ \bullet \\ \bullet \\ \bullet \\ y_p \end{bmatrix} - \begin{bmatrix} h_{11} & \bullet & \bullet & h_{1p} \\ \bullet & & & \\ \bullet & & & \\ \bullet & & & \\ \bullet & & & \\ h_{p1} & \bullet & \bullet & h_{pp} \end{bmatrix} \begin{bmatrix} x_1 \\ \bullet \\ \bullet \\ \bullet \\ \bullet \\ x_p \end{bmatrix} \right\|^2$$

**Figure 2.16** ML detection equation (number of transmitter antennas =  $p$ )

This algorithm steps and notations can be illustrated as follows:

*Notation:*

$\hat{x}_1, \hat{x}_2, \dots, \hat{x}_p$  : the estimated values.

$\Theta$  : finite set, such as BPSK, QPSK, and 16-QAM

$y_{[1,2,\dots,p]}$  : nulling from the  $p$ -th to  $n$ -th row of  $y$ .

$[x_1, x_2, \dots, x_p]$  : the transmitted symbols.

$H_{[1,2,\dots,p]}$  : the channel matrix's 1 ~  $p$  columns.

*Step 1:*

*adopt ZF V-BLAST method to get initial decision values.*

*Step 2:*

*adopt the ML method for the first 1~ $p$  subchannels, based on the cost function*

$$\{\hat{x}_1, \hat{x}_2, \dots, \hat{x}_p\} = \arg \min_{\hat{x}_1, \hat{x}_2, \dots, \hat{x}_p \in \Theta} |y_{[1,2,\dots,p]} - H_{[1,2,\dots,p]}[x_1 \dots x_p]| \quad (2.19)$$

*Step 3:*

*combine the outputs of step 1 and step 2.*

*Step 4:*

*adopt ZF V-BLAST method to modify the output of step 3.*

This algorithm reduces the ML detection in Figure 2.15 to Figure 2.16. But  $p$  is hard to choose from design equation [23]. However, in most case one will not use too many receiver antennas. Hence this approach is feasible. This approach must combine V-BLAST technique and ML detection with modification. Still, it is not clear about the modification. However, this approach gives us some thought about hybrid ML detection and V-BLAST detection in Chapter 3.

### 2.3.3.3 The MMSE-BLAST Detection Method

The way to improve detection performance especially for mid-range SNR values is to replace the ZF nulling operations proposed in [24] with the more effective minimum mean-square error (MMSE) algorithms as shown by equation (2.20).

$$G_{ZF} = (H^H H + \sigma_n)^{-1} H^H \quad (2.20)$$



### 2.3.3.3.1 Modified Channel Matrix on the Performance of MMSE V-BLAST Technique

In [25], the authors propose a MMSE detection algorithm that exterminates mutual interferences. Hence BER performance is improved. The detection is done by changing the channel matrix after each detection step. The authors also verify the analysis after simulations. Through equation substitution we will compare the mentioned three methods including ZF method, MMSE method [24], and the modified MMSE [25].

In ZF criterion, at the  $k_i$ -th detection stage because of the orthogonal property between  $(G)_{k_i}$  and  $(H)_{k_i}$ , we have the following result

$$(G)_{k_i} y = (G)_{k_i} (Hx + n) = (G)_{k_i} Hx + (G)_{k_i} n = \alpha x + (G)_{k_i} n \quad (2.21)$$

where  $\alpha = [0, 0, \dots, 1, \dots, 0]$ , whose elements are all zero except the  $k_i$ -th position. On the contrary, in the MMSE nulling operation it is not complete zero, and  $\alpha$  is given by

$$\alpha = [\alpha_{k_1}, \alpha_{k_2}, \dots, \alpha_{k_i}, \dots, \alpha_{k_j}, \dots, \alpha_{k_{N_t}}], \text{ where } \alpha_{k_i} \neq 0 \quad (2.22)$$

The idea here is to reduce interference before the  $k_i$  sub-stream. The  $k_{i-1}$ -th element of  $(G)_{k_i}$  is also zero. As a result, the product vector  $\alpha$  is found to be

$$\alpha = [0, 0, \dots, 0, \alpha_{k_i}, \dots, \alpha_{k_j}, \dots, \alpha_{k_{N_t}}] \quad (2.23)$$

In conclusion, the interference from the detected sub-stream is suppressed. The method can be summarized as follows.

$$H^1 = H$$

$$y_1 = y$$

$$k_i \leftarrow 1$$

for ( $i=1; i \leq N_t; i++$ )

$$G = (H^H H + \alpha_n^2 I_{n_i})^{-1} H^H$$

$$k_i = \arg_i \min \|G\|$$

$$\hat{x}_{k_i} = (G)_{k_i} y$$

$$x_{k_i} = \text{quantize} \left( \hat{x}_{k_i} \right)$$

$$y = y - x_{k_i} (H)_{k_i}$$

$$(H)_{k_i} = 0$$

$$k_{i+1} \leftarrow k_i$$

*end*

### 2.3.3.4 V-BLAST Technique with Parallel Symbol Cancellation

Golden's detection process [9] uses techniques of linear-combination nulling and successive symbol cancellation. Like conventional successive symbol cancellation (SSC), Golden's detection algorithm has long time delay. Moreover, the larger the number of transmit antennas, the longer detection delay. Aiming at this problem, a detection algorithm based on parallel symbol cancellation (PSC) is proposed in [26].

#### 2.3.3.4.1 Two-Stage V-BLAST Detection Algorithm

In order to avoid long time delay, parallel symbol cancellation (PSC) was proposed [26]. However the performance will be degraded. To reduce the problem, this two-stage algorithm combines SSC with PSC techniques so as to improve the BER performance. The proposed scheme is combined with ZF technique. The algorithm is divided into two distinct stages.

Stage1: use V-BLAST method to obtain a good initial decision.

Stage2: use parallel symbol cancellation to attain the estimated value of the transmitted vector.

The proposed algorithm based on ZF criterion is described below:

Stage 1: initialization

$$i = 1$$

$$G_1 = H^+$$

$$k_1 = \arg \min_j \|(G_1)_j\|^2$$

for ( $i=1; i \leq N_t; i++$ )

$$x_{k_i,0} = (G_i)_{k_i} y_i$$

$$\hat{x}_{k_i,0} = Q(x_{k_i,0})$$

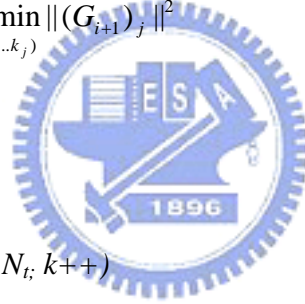
$$y_{i+1} = y_i - \hat{x}_{k_i,0} (H)_i$$

$$(H)_{k_i} = 0$$

$$(G)_{i+1} = H_{k_i}^+$$

$$k_{i+1} = \arg \min_{j \notin (k_1 \dots k_i)} \|(G_{i+1})_j\|^2$$

end



Stage 2: initialization

for ( $k=1; k \leq N_t; k++$ )

$$k = 1$$

$$\hat{x}_{n,0} = \hat{x}_{k_i,0} \quad (n = 1, 2, 3, \dots, n_t)$$

$$y_{n,k} = y - \sum_{i=1, i \neq n}^{n_t} \hat{x}_{i,k-1} (H)_i \quad (n = 1, 2, 3, \dots, n_t) \quad (2.24)$$

$$x_{n,k} = (G)_n y_{n,k}$$

$$\hat{x}_{n,k} = Q(x_{n,k})$$

$$(G)_n = [(H)_n]^+$$

end

Equation (2.24) can obtain a diversity order equals the receiver antennas. We will compare this method with the proposed algorithm in Chapter 3.

### 2.3.4 Complexity Comparisons of Data Detection Algorithms

The 0th-order simplified detection denotes the approach of copied vectors in Section 2.3.3.1. The 1st-order simplified Detection (approximation) denotes is mentioned in section 2.3.3.1. Shen's and Li's iterative methods [19] are discussed in Section 2.3.3.2.1. Akhtar's method [22] denotes the new K approach in Section 2.3.3.2.2, Baro's method [23] denotes joint ML and DFE scheme in Section 2.3.3.2.3, Duong's method [25] denotes the approach with modified channel matrix in Section 2.3.3.3.1, while Xiaofeng's method [26] denotes the PSC method in Section 2.3.3.4.1.

Although complexity of the 0th-order simplified detection method is smaller than the others, it only saves 20% simulation time. For Shen's and Li's iterative methods, their performances are similar. However the Li's iterative method can get more diversity order. Baro's method is complicated, because it must do V-BLAST detection and ML detection. Moreover, it must compute  $p$ , which is hard to solve. That is not feasible. Xiaofeng's PSC method must detect signal at the same time, so it need many parallel ZF and PSC units [28].

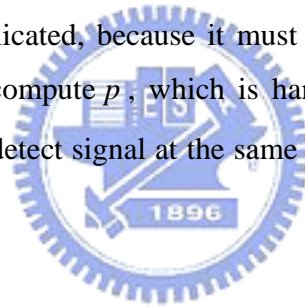


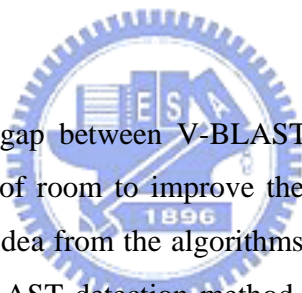
**Table 2.4** Complexity comparisons of data detection algorithms

	No. Multiplication	$N_t = 4, N_r = 4$ QPSK(A=4)
V-BLAST	$N_t^4 + 2N_t^3N_r + N_t^2N_r + (N_t^2 + N_tN_r) \times 6$	1024
ML	$A^{N_t}N_r(N_t + 1)$	5120
Simplified Detection (0th-order appr.)	$(N_t^2 + N_tN_r) \times 6$	192
Simplified Detection (1st-order appr.)	$2N_t^2N_r + (N_t^2 + N_tN_r) \times 6$	320
Shen's iterative method [19]	$N_t^4 + 2N_t^3N_r + N_t^2N_r + (N_t^2 + N_tN_r) \times 6 + \frac{N_tN_r(N_t + 1)}{2} + \frac{N_t(N_t + 1)(2N_t + 1)}{6}$	1094
Li's iterative method [21]	$N_t^4 + 2N_t^3N_r + N_t^2N_r + (N_t^2 + N_tN_r + (N_t - 1)^2 + (N_t - 1)N_r) \times 6$	1150
Akhtar's changing $k$ method [22]	$N_t^4 + 2N_t^3N_r + N_t^2N_r + 12N_t^2 + (N_t^2 + N_tN_r) \times 6$	1216
Baro's joint ML and DFE method [23]	$N_t^4 + 2N_t^3N_r + N_t^2N_r + (N_t^2 + N_tN_r) \times 6 + A^p N_p (N_p + 1)$ ( $p$ is chosen from [8].)	768+ $A^p N_p (N_p + 1)$
Duong's modified $H$ method [24]	$N_t^4 + 2N_t^3N_r + N_t^2N_r + (N_t^2 + N_tN_r) \times 6$	1024
Xiaofeng's PSC method [25]	$N_t^4 + 2N_t^3N_r + N_t^2N_r + (N_t^2 + N_tN_r) \times 6 + (3N_t^2 + N_tN_r) \times 6$	1408



# Chapter 3

## The Proposed Data Detection Algorithms



Since the performance gap between V-BLAST detection and ML detection is significant, we still have a lot of room to improve the V-BLAST techniques. Through technique survey we got some idea from the algorithms in Chapter 2. We will propose a hybrid ML detection and V-BLAST detection method in this chapter. The method will reduce a great deal of the comparison operations in ML detection. It will get better performance than V-BLAST method, without increasing too many comparison operations. Besides, it will decrease complex multiplication in calculating pseudo-inverses.

### 3.1 The New Detection Methods

As we know joint ML and V-BLAST can get better performance, it provides an idea for further improvement. Specifically, after the initial values  $x_1$  to  $x_{N_t}$  are detected, we can use further other detection method like ML detection to do the detection again.

First, let us suppose  $N_t$  transmitter antennas and  $N_r$  receiver antennas. If we use QPSK modulation, and want to detect the transmitted signals, then a total of  $(N_t)^4$

comparisons will have to be made. Generally, in detecting M-QAM by using ML method, a total of  $(N_t)^M$  comparisons need to be made.

We suppose that some of signals are already known. As such, in this way we don't need to do all the comparisons and it will decrease a large number of comparison operations in ML detection, while still maintain good performances.

### 3.1.1 New Hybrid ML and V-BLAST Detection Method

As mentioned before, one can reduce the complexity of equation (2.8), if we already know some detected signals. For example if in  $M$ -PSK modulation there is only one unknown symbol, then we just only need to compare  $M$  values in ML detection. Based on the idea, first V-BLAST method is used to detect all the initial values, and then we update it by ML detection. Suppose  $L$  is the level we want to do the detection, ranging from 1 to  $N_t$ . In other word, we will update  $L$  value by ML detection.

The algorithm is summarized below and shown in Figure 3.1:

*Step 1:*

*adopt V-BLAST method to get the initial  $\hat{x}_1' \dots \hat{x}_{N_t}'$  values*

*Step 2:*

*Based on the known  $\hat{x}_1' \dots \hat{x}_{N_t}'$  values, update  $\hat{x}_1' \dots \hat{x}_L$  values by ML*

*detection  $\{\hat{x}_L\} = \underset{\hat{x}_L \in \Theta}{\operatorname{argmin}} |y - [x] \bullet (H)|$ , and the other values (i.e.*

*$\hat{x}_{L+1}' \dots \hat{x}_{N_t}'$ ) by V-BLAST detection*



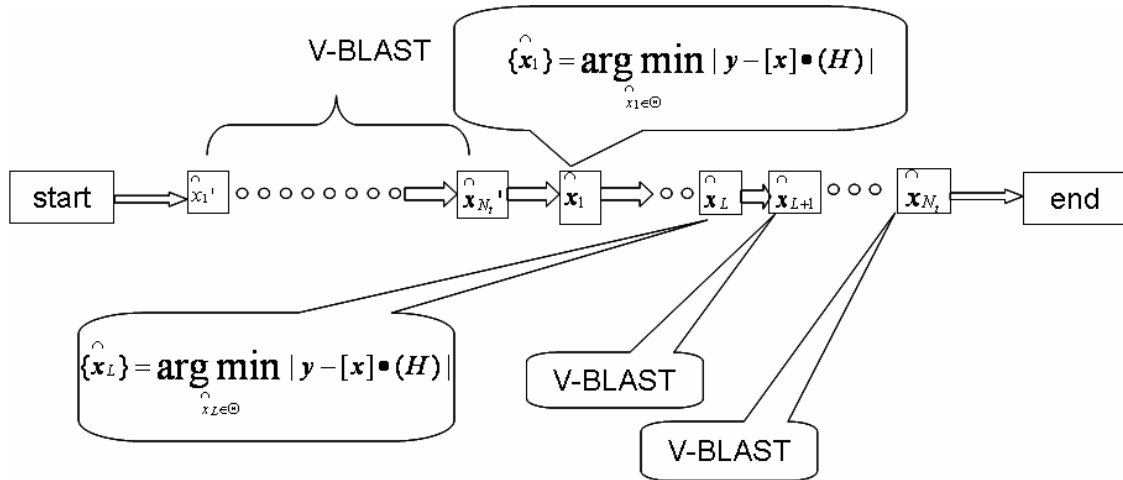


**Figure 3.1** The proposed hybrid ML and V-BLAST detection

For illustration, we show the detection flow for  $L = 1$  and  $L = N_t$  in Figure 3.2 and

Figure 3.3, respectively.

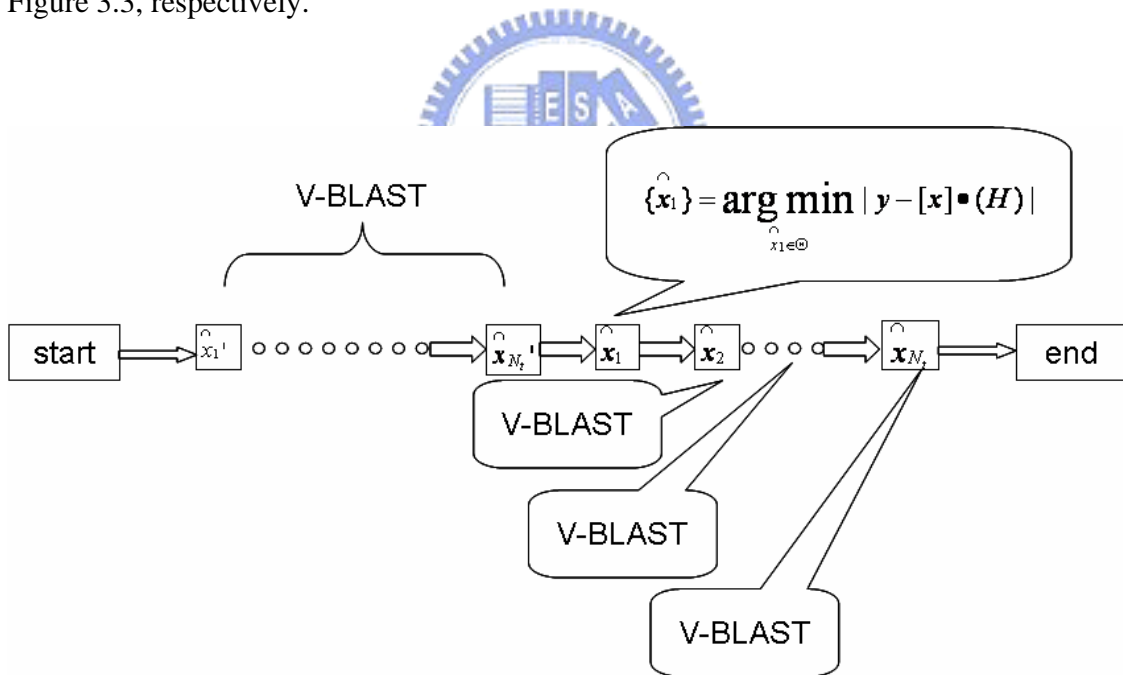


**Figure 3.2** The proposed hybrid ML and V-BLAST detection (simplest case for  $L = 1$ )

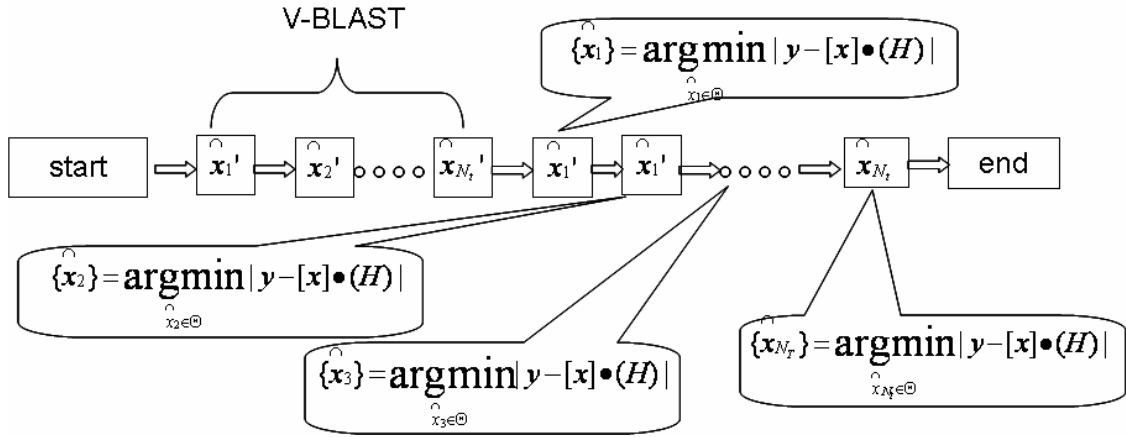


**Figure 3.3** Flow diagram of the proposed hybrid ML and V-BLAST detection (the most complex case,  $L = N_t$ )

In this approach we can confine error propagation, meantime reduce computation complexity. For ML detection, the number of minimum norm we calculate ranging from  $(N_t)^M$  to  $L \times N_t$  ( $\Theta$  is M-QAM). We will discuss complexity of the proposed design in Section 3.4 and verify its in Chapter 4.

### 3.1.2 Extension of the new method

When a system has a large number of transmitter antennas, we can use this approach to detect two or more values at the same time. But here we only discuss the case of detecting two values at the same time. Figure 3.4 depicts the algorithm flow as shown below. The algorithm is summarized below:

*Step1:*

*adopt V-BLAST to get the initial  $\hat{x}_1, \dots, \hat{x}_{N_t}$  values*

*Step2:*

with the detected  $\hat{x}_1' \dots \hat{x}_{N_t}'$  values in Step1, update  $\hat{x}_1', \hat{x}_2'$  by ML detection based on  $\{\hat{x}_1, \hat{x}_2\} = \arg \min_{\hat{x}_1, \hat{x}_2 \in \Theta} |y - [x] \bullet (H)|$  also update the other values  $\{\hat{x}_3, \hat{x}_4\}, \{\hat{x}_5, \hat{x}_6\} \dots \{\hat{x}_{N_t-1}, \hat{x}_{N_t}\}$  using similar method

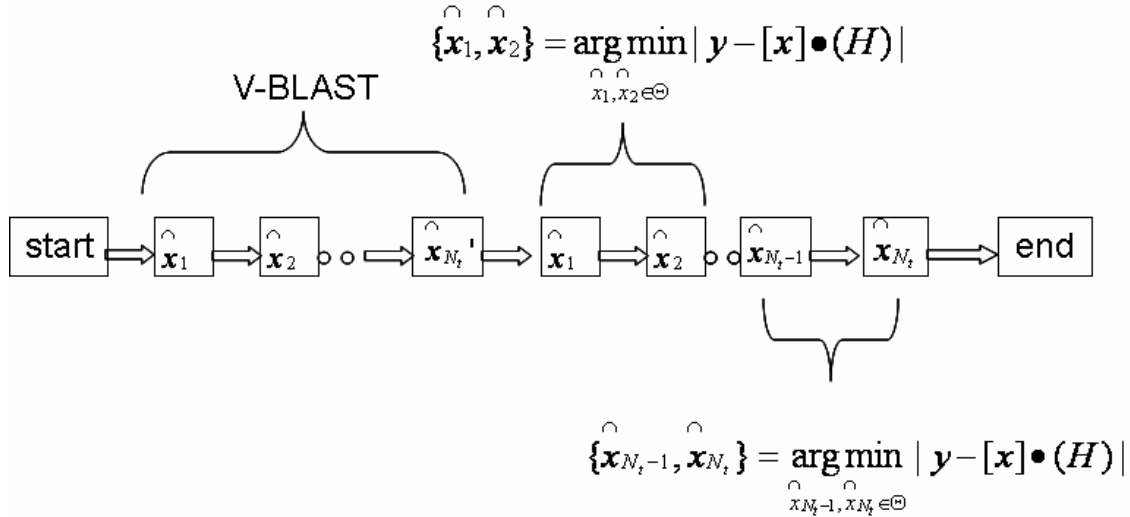


Figure 3.4 Extension of the proposed algorithm



Although the proposed extended method can get better performance than the proposed method in section 3.1.1, will increase complexity. The complexity will be discussed in section 3.4.

## 3.2 The Compared Detection Techniques

### Li's and Shen's methods [19,21]

In 2.3.3.2.1 we introduce these two iterative detection methods, which have similar performances and complexities. In Chapter 4 we will compare Li's and Shen's methods in simulation.

## Our Improved Li's method

Shen's method focuses on optimizing diversity order. It increases diversity order in second loop to get better performance than V-BLAST method. Here, we can modify the Li's method and increase its diversity order. Precisely equation (3.2) will be used to increase diversity order in the second loop. Therefore, in second loop all the signals will have  $N_t$  diversity orders. The algorithm steps are shown below. ( $\tilde{H}_{i-1}$  means the resulting  $\tilde{H}$  matrix after nulling the  $i-1$ th column of  $\tilde{H}$ )

Step 1:

Perform the optimal ordering and SIC according to V-BLAST method and get the detected symbols  $\hat{x}_1^{old}, \hat{x}_2^{old}, \dots, \hat{x}_{N_t}$  (the optimal order is assumed to be  $1, 2, \dots, N_t$ ).

Step 2:

$$\tilde{H} = H$$

$$\tilde{y} = y; \hat{x}_{N_t}^{new} = \hat{x}_{N_t}$$

for  $i = N_t - 1$  to 1

$$\tilde{y} = \tilde{y} - \sum_{i=1, i \neq n}^{n_t} \hat{x}_i \tilde{H}_{i-1} \quad (n = 1, 2, 3, \dots, n_t) \quad (3.2)$$

$$\tilde{H} = \tilde{H}_{i-1};$$

$$\hat{x}_i = (\tilde{H}^+)_i \cdot \tilde{y}$$

$$\hat{x}_i = Q(\hat{x}_i)$$

End

## 3.3 Reducing Computational Complexities in Pseudo-Inverse

If  $H$  is a  $m \times n$  matrix, then  $(H^H H)^H = (H^H)^H H^H = H H^H$ , and  $H^H H$  is Hermitian [27]. We can simply compute the elements above diagonal and those below

diagonal are their complex conjugate. In this way we can save some multiplication and addition complexities.

Suppose the transmitter has  $N_t$  antennas and receiver has  $N_r$  antennas, then  $H^H H$  is  $N_t$  by  $N_t$ . Normally, the required number of multiplication operation  $H^H H$  is  $(N_t)^3$ . However, considering the mentioned symmetry one can save

$N_t(1 + N_t - 1) \times (N_t - 1) = (N_t)^2 \times (N_t - 1) = \frac{N_t^2(N_t - 1)}{2}$  multiplication operations. The complexity reduction ratio is  $\frac{N_t^2(N_t - 1)}{2(N_t)^3} = \frac{(N_t - 1)}{2N_t}$ . If  $N_t = 4$ , the ratio is  $\frac{3}{8}$ , and if

$N_t = 6$  the ratio is  $\frac{5}{12}$ . The simplification skill is used in the simulations of Chapter 4.

$$\begin{aligned}
 H^H H &= \begin{bmatrix} H_{11} & H_{12} & \dots & H_{1N_t-1} & H_{1N_t} \\ H_{21} & H_{22} & \dots & H_{2N_t-1} & H_{2N_t} \\ \dots & \dots & \dots & \dots & \dots \\ \dots & \dots & \dots & H_{N_t-1N_t-1} & H_{N_t-1N_t} \\ H_{N_t1} & H_{N_t2} & \dots & H_{N_tN_t-1} & H_{N_tN_t} \end{bmatrix} \\
 &= \begin{bmatrix} H_{11} & H_{12} & \dots & H_{1N_t-1} & H_{1N_t} \\ H_{12}^* & H_{22} & \dots & H_{2N_t-1} & H_{2N_t} \\ \dots & \dots & \dots & \dots & \dots \\ \dots & \dots & \dots & H_{N_t-1N_t-1} & H_{N_t-1N_t} \\ H_{1N_t}^* & H_{2N_t}^* & \dots & H_{N_t-1N_t}^* & H_{N_tN_t} \end{bmatrix}
 \end{aligned}$$

Figure 3.5 Hermitian symmetry of matrix  $H^H H$

### 3.4 Complexity Analysis and Comparison

In this section, we will compare the multiplication complexities of the proposed technique with those of V-BLAST detection, ML detection, and the two methods in section 3.2. Table 3.1 shows the approximate multiplication complexities which roughly fit the simulation time complexities as will be shown in Chapter 4. Multiplication complexities of various detection algorithms for V-BLAST's channel inversion are  $N_t^4 + 2N_t^3N_r + N_t^2N_r$ , and for data detection are  $N_t^2 + N_t$ .

From Table 3.1 we know that the ML detection is roughly six-times complicated than that of V-BLAST method. The complexity of the proposed method ( $L=1$ ) is similar to V-BLAST. But its performance is better than V-BLAST method. Chapter 4 will verify the performances. Table 3.2 considers the matrix symmetry.

**Table 3.1** Multiplication complexities of various detection algorithms without considering matrix symmetry

	No of Multiplications	$N_t=4, N_r=4$ (or 5,6) QPSK(A=4)
V-BLAST	$N_t^4 + 2N_t^3N_r + N_t^2N_r + (N_t^2 + N_tN_r) \times 6$	1024
ML	$A^{N_t}N_r(N_t + 1)$	5120
Shen's method	$N_t^4 + 2N_t^3N_r + N_t^2N_r + (N_t^2 + N_tN_r) \times 6 + \frac{N_tN_r(N_t + 1)}{2} + \frac{N_t(N_t + 1)(2N_t + 1)}{6}$	1094
Li's method	$N_t^4 + 2N_t^3N_r + N_t^2N_r + (N_t^2 + N_tN_r + (N_t - 1)^2 + (N_t - 1)N_r) \times 6$	1150
Our Improved Li's method	$N_t^4 + 2N_t^3N_r + N_t^2N_r + (N_t^2 + N_tN_r + 2(N_t - 1)^2 + (N_t - 1)N_r) \times 6$	1204
Proposed method ( $L=1$ )	$N_t^4 + 2N_t^3N_r + N_t^2N_r + (N_t^2 + N_tN_r + (N_t - 1)^2 + (N_t - 1)N_r) \times 6 + AN_r(N_t + 1)$	1230
Proposed method ( $L=N_t$ )	$N_t^4 + 2N_t^3N_r + N_t^2N_r + (N_t^2 + N_tN_r) \times 6 + 4AN_r(N_t + 1)$	1344
Proposed extended method (two values at a time)	$N_t^4 + 2N_t^3N_r + N_t^2N_r + (N_t^2 + N_tN_r) \times 6 + 2A^2N_r(N_t + 1)$	1664

**Table 3.2** Multiplication complexities of various detection algorithms, considering matrix symmetry

	No. of Multiplications	$N_t=4, N_r=4$ (or 5,6) QPSK(A=4)
V-BLAST	$N_t^4 + 2N_t^3N_r + N_t^2N_r + (N_t^2 + N_tN_r) \times 6 - N_tN_r(N_t - 1)/2$	1000
ML	$A^{N_t}N_r(N_t + 1)$	5120
Shen's method	$N_t^4 + 2N_t^3N_r + N_t^2N_r + (N_t^2 + N_tN_r) \times 6 + \frac{N_tN_r(N_t + 1)}{2} + \frac{N_t(N_t + 1)(2N_t + 1)}{6} - N_tN_r(N_t - 1)/2$	1070
Li's method	$N_t^4 + 2N_t^3N_r + N_t^2N_r + (N_t^2 + N_tN_r + (N_t - 1)^2 + (N_t - 1)N_r) \times 6 - N_tN_r(N_t - 1)/2$	1126
Our Improved Li's method	$N_t^4 + 2N_t^3N_r + N_t^2N_r + (N_t^2 + N_tN_r + 2(N_t - 1)^2 + (N_t - 1)N_r) \times 6 - N_tN_r(N_t - 1)/2$	1180
Proposed method (L=1)	$N_t^4 + 2N_t^3N_r + N_t^2N_r + (N_t^2 + N_tN_r + (N_t - 1)N_r + AN_r(N_t + 1)) \times 6 - N_tN_r(N_t - 1)/2$	1206
Proposed method (L=N <sub>t</sub> )	$N_t^4 + 2N_t^3N_r + N_t^2N_r + (N_t^2 + N_tN_r) \times 6 + 4AN_r(N_t + 1) - N_tN_r(N_t - 1)/2$	1320
Proposed extended method (two values at a time)	$N_t^4 + 2N_t^3N_r + N_t^2N_r + (N_t^2 + N_tN_r) \times 6 + 2A^2N_r(N_t + 1) - N_tN_r(N_t - 1)/2$	1640





# Chapter 4

## Simulation Results

In this chapter, we conduct computer simulations and test the performances of the discussed algorithms in Chapters 2 and 3 by using Matlab programs. Those simulations are performed according to EWC 802.11n specifications. Table 4.1 lists the parameter settings of EWC used in the simulations including frame structure, multi-antenna preambles format, signal bandwidth, subcarrier number, et cetera. Modulation scheme is fixed to QPSK and channel coding is neglected. It is also assumed that channel state information (CSI) is perfectly known during the periods of preambles.

First of all, based on the previously mentioned complexity analysis, simulation time is examined. Then bit error rates (BER) are simulated.

Table 4.1 Simulated EWC 802.11n system parameters

Signal bandwidth	20MHz
Sample duration	50ns
FFT length	64
Used subcarriers	52
Data subcarriers	48
Symbol period	3.2 $\mu$ s (64 samples)
Cyclic prefix	0.8 $\mu$ s (16 samples)
Subcarrier spacing	312.5 kHz
Modulation	QPSK
Channel Coding	No
Transmit antenna	2, 3, or 4
Receive antenna	4, 5, or 6
Data symbol	6 symbols
Doppler frequency	150 Hz( 9m/s at 5GHz )

## 4.1 Performance – Execution Time

In the following figures, computation time is measured in seconds using Matlab elapse time functions. Only signal detection is measured and other parts are not, because we are only interested in complexities of detections. 4 transmit and 4, 5, and 6 receive antennas are assumed.

In Figure 4.1, the fractional numbers represent the ratio normalized to the methods of V-BLAST, Li's method, Shen's method, our improved Li's method, ML1 (the proposed method  $L=1$ ), ML2 (the proposed method  $L=2$ ), ML3 (the proposed method  $L=3$ ), ML4 (the proposed method  $L=4$ ), ML two values (the new extended method) and ML detection. For simplicity, the proposed methods assuming ( $L=1\sim Nt$ ) will be discussed separately. Therefore, from figures we can judge which one has better performance and less cost.

From Figures 4.1 to 4.3, the ratios of simulation time are roughly equal to Table 3.2 and Table 4.2. The proposed method's ( $L=1$ ) simulation time is 1.1 times the length of the V-BLAST method. As shown, ML method is very time consuming.

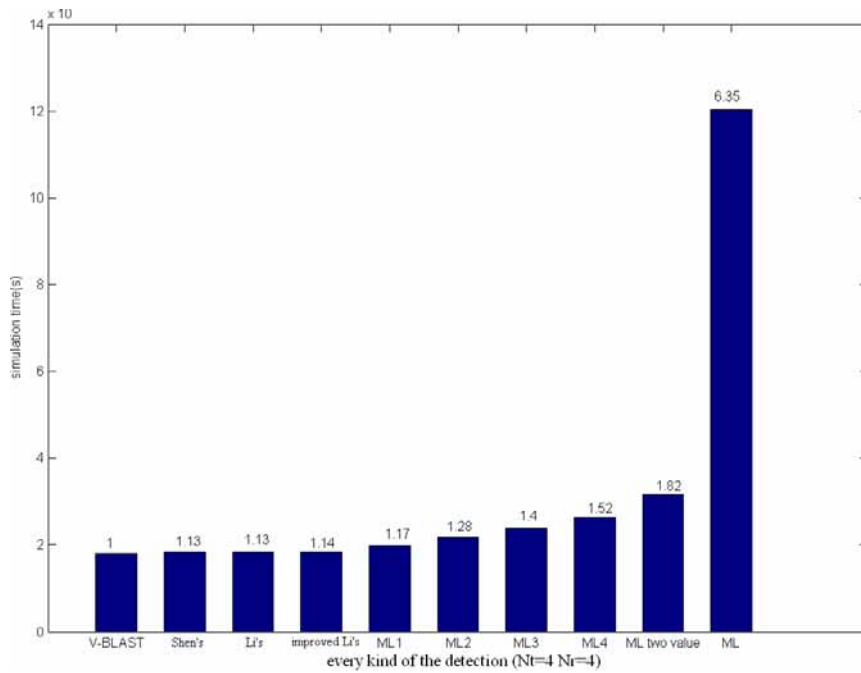


**Figure 4.1** Computation time comparison of existing detection methods and the proposed methods ( $N_t=4$   $N_r=4$ )

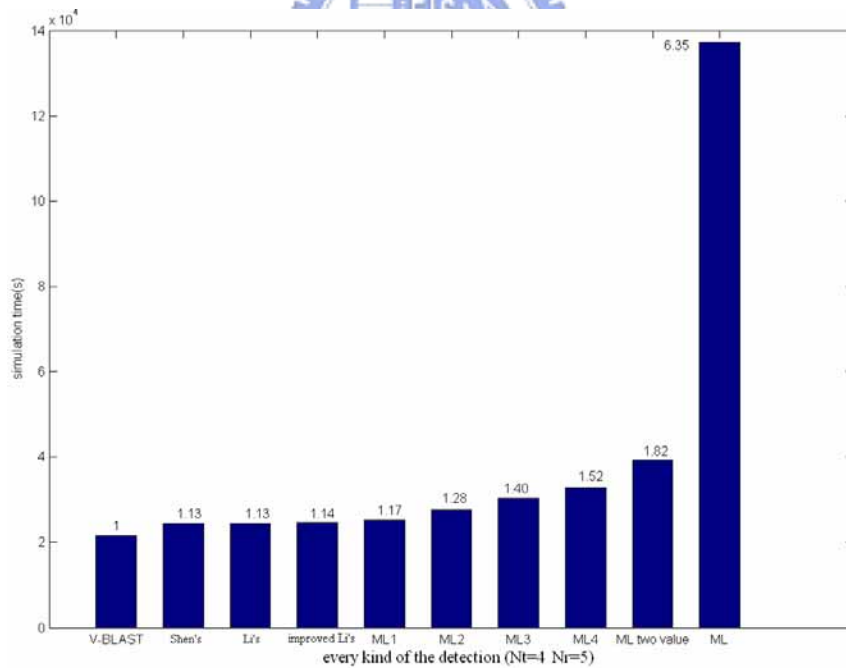


**Figure 4.2** Computation time comparison of the existing detection methods and the proposed methods ( $N_t=4$   $N_r=5$ )

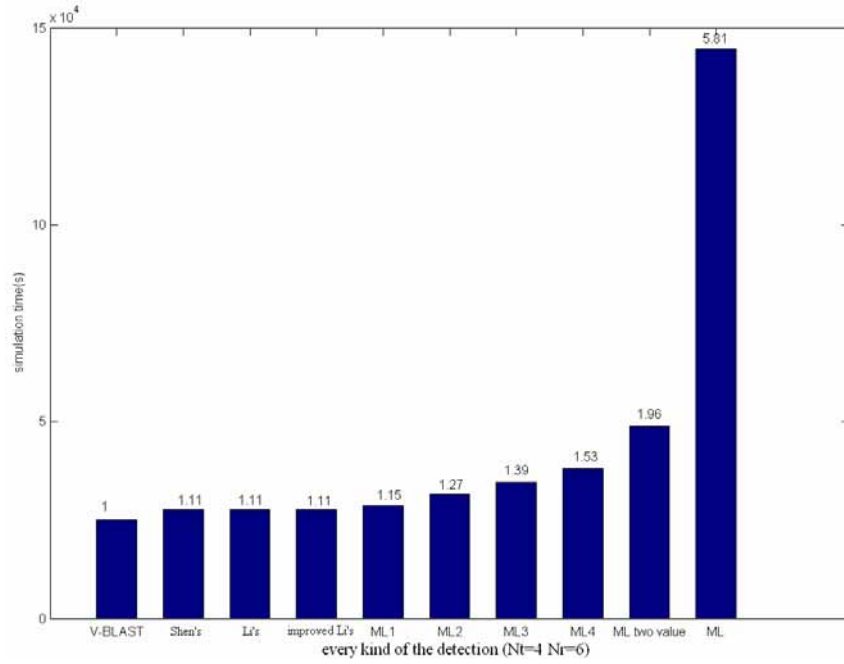


**Figure 4.3** Computation time comparison of the existing detection methods and the proposed methods ( $N_t=4$   $N_r=6$ )

**Table 4.2** Multiplication complexities of the proposed detection algorithms vs.  $L$  value, considering matrix symmetry

$L$	No. of Multiplications	$N_t=4, N_r=4$ QPSK(A=4)
1	$N_t^4 + 2N_t^3N_r + N_t^2N_r + (N_t^2 + N_tN_r + (N_t - 1)^2 + (N_t - 1)N_r) \times 6 + AN_r(N_t + 1) - N_tN_r(N_t - 1)/2$	1206
2	$N_t^4 + 2N_t^3N_r + N_t^2N_r + (N_t^2 + N_tN_r + (N_t - 2)^2 + (N_t - 2)N_r) \times 6 + 2AN_r(N_t + 1) - N_tN_r(N_t - 1)/2$	1232
3	$N_t^4 + 2N_t^3N_r + N_t^2N_r + (N_t^2 + N_tN_r + (N_t - 3)^2 + (N_t - 3)N_r) \times 6 + 3AN_r(N_t + 1) - N_tN_r(N_t - 1)/2$	1270
4	$N_t^4 + 2N_t^3N_r + N_t^2N_r + (N_t^2 + N_tN_r) \times 6 + 4AN_r(N_t + 1) - N_tN_r(N_t - 1)/2$	1320

## 4.2 Performance – Bit Error Rate

In our discussion, correlations between transmit antennas and receive antennas are assumed independent, and each transmit and receive antenna pair has the same channel model. In the BER simulations, indoor channel model [28] is adopted, because both EWC 802.11n and 802.11a assume similar indoor wireless applications, and the simulated channel is generated by a hand-written program using Jake's model. Besides, the correlation between any of the two taps of the models is small. As shown before, a simulated packet consists of the preamble part and 6 data symbols. In our simulation, perfect channel state information (CSI) is assumed.

The first simulated channel, as listed in Table 4.3, is measured in a typical old office environment where partitions are often made of bricks. The longest tap has a delay of 127ns, which is about 2.5 samples for 802.11a system. The delay is so small that a very large coherent bandwidth is expected.

**Table 4.3** Indoor channel model [28] with short delays, office environment

Tap No.	Delay (ns)	Power (dB)	Amplitude Distribution	Doppler Spectrum
1	0	0	Rayleigh	Classical/Flat
2	36	-5	Rayleigh	Classical/Flat
3	84	-13	Rayleigh	Classical/Flat
4	127	-19	Rayleigh	Classical/Flat

Figure 4.4 shows performances of various techniques, where 2x2 means that there are 2 transmit and 2 receive antennas. ML denotes ML detection, V-BLAST denotes V-BLAST detection, Shen's denote Shen's method, Li's denotes Li's method [22] in section 3.2, improved Li's denotes our improved Li's method in section 3.2, ML1 denotes  $L=1$  in section 3.1.1, ML2 denotes  $L=2$  in section 3.1.1, ML3 denote  $L=3$  in section 3.1.1, ML4 denote  $L=4$  in section, ML\_ext denote the new extended method (detect two values) at a time in section 3.1.2. In Figure 4.5, 2x3 means that there are 2 transmit and 3 receive antennas, similarly for Figure 4.6. ML1 to ML4 are compared separately in Figure 4.13.

It is obvious that the proposed method ( $L=1$ )  $N_t = N_r$ , has better performance than V-BLAST, with little increase in complexity. And in the figures there is no performance difference between V-BLAST algorithms and comparison algorithms. The condition is also observed in Figure 4.5 and Figure 4.6. Figure 4.7, 4.8, and 4.9 are for the case of 3 transmitter antennas 3, 4, and 5 receiver antennas, respectively.

In each figure the performance of the V-BLAST, Shen's method, Li's method, and our improved Li's method are the same. The reasons are that algorithm of the Li's method in section 2.3.3.2.1 [21] channel response  $H$  are the same in Step 1 and Step 2. The difference is just the part of data detection is recomputed, but  $H$  are the same. And in [21] the approach is fit to use in ideal detection and cancellation. When the error propagation exists the performance of every detected layer are very close. Hence Li's method has no effect in enhancing performance here. The performances of Shen and Li's method are the same. And its reason and Li's method are the same.

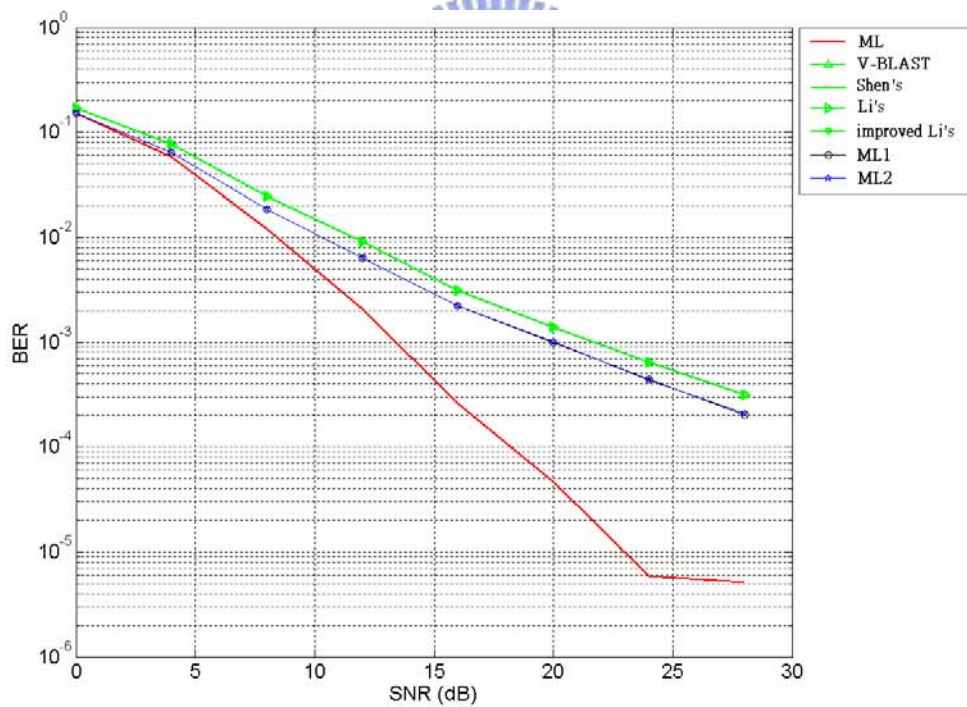


**Figure 4.4** BER performance versus SNR of various detection techniques (2x2), office environment

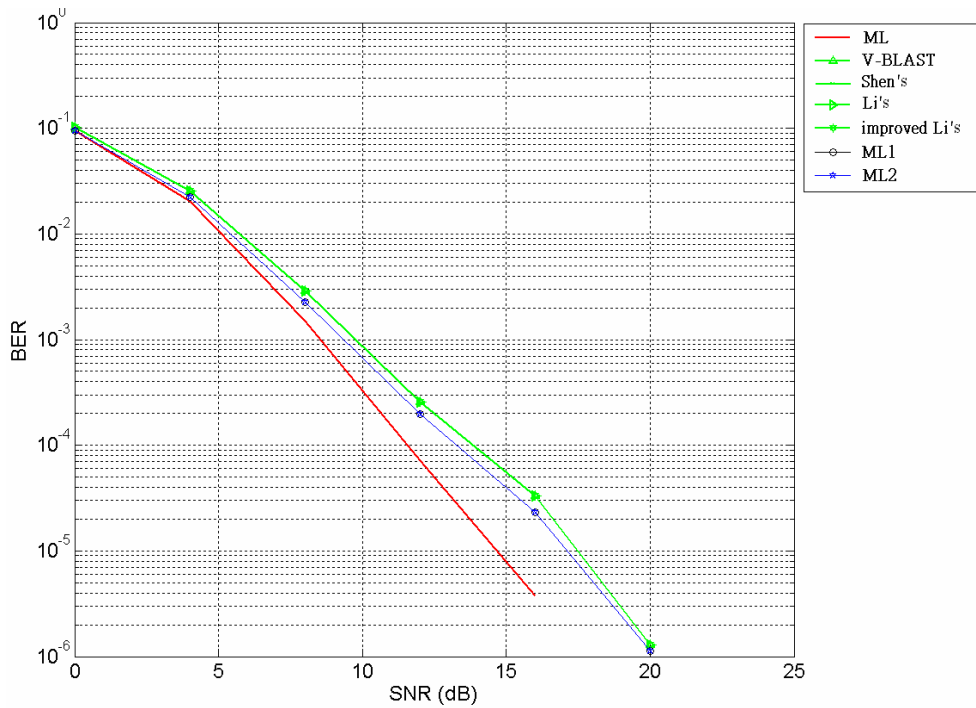


**Figure 4.5** BER performance versus SNR of various detection techniques (2x3), office environment

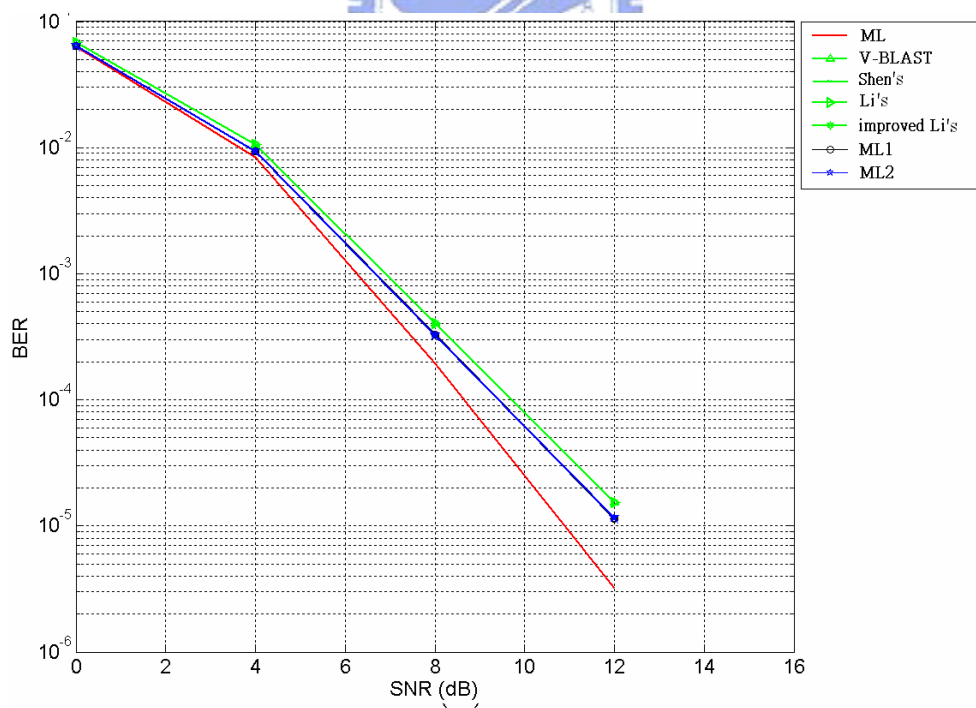


**Figure 4.6** BER performance versus SNR of various detection techniques (2x4), office environment

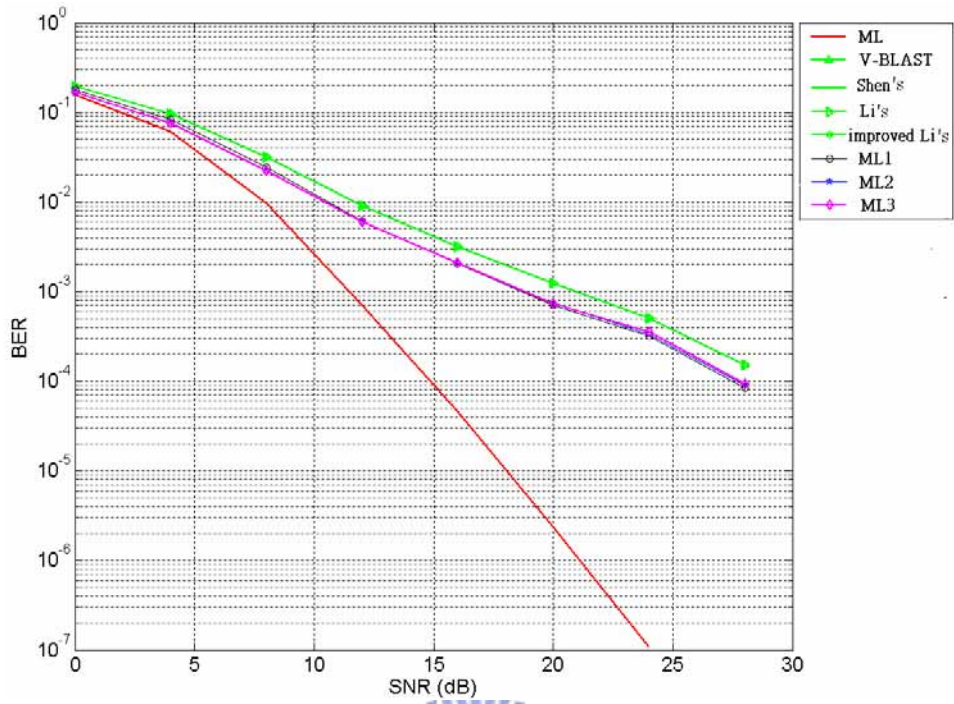


**Figure 4.7** BER performance versus SNR of various detection techniques (3x3), office environment

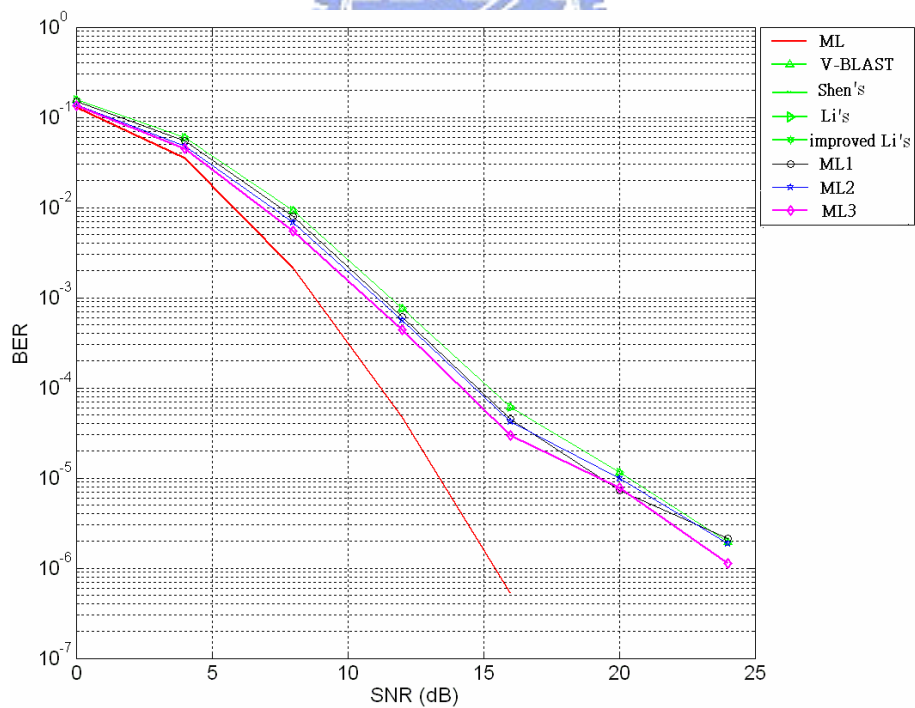


**Figure 4.8** BER performance versus SNR of various detection techniques (3x4), office environment



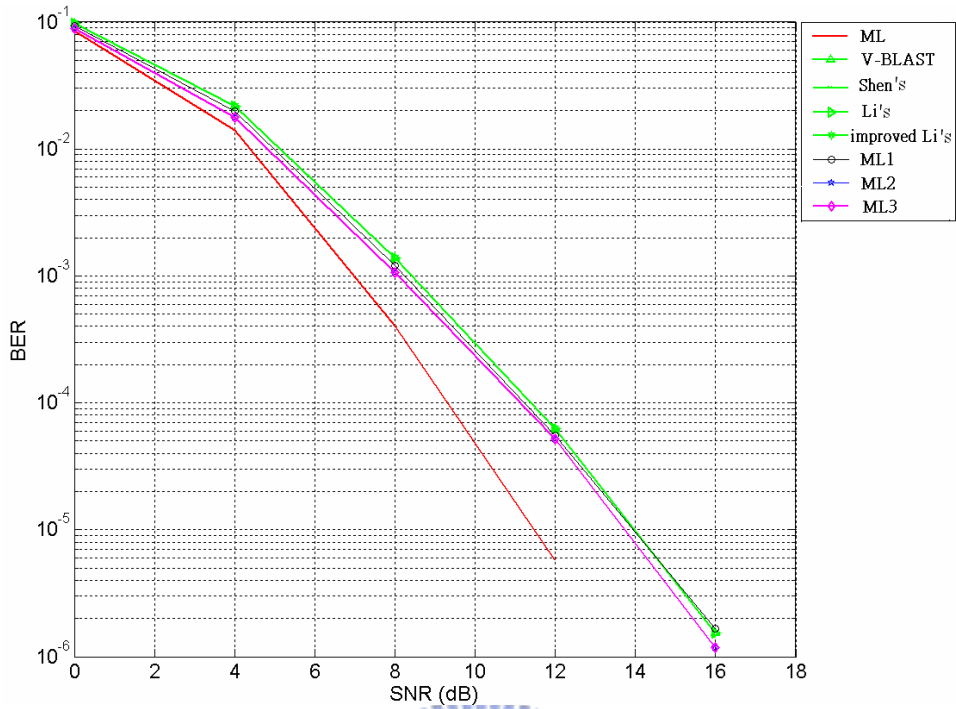


**Figure 4.9** BER performance versus SNR of various detection techniques (3x5), office environment

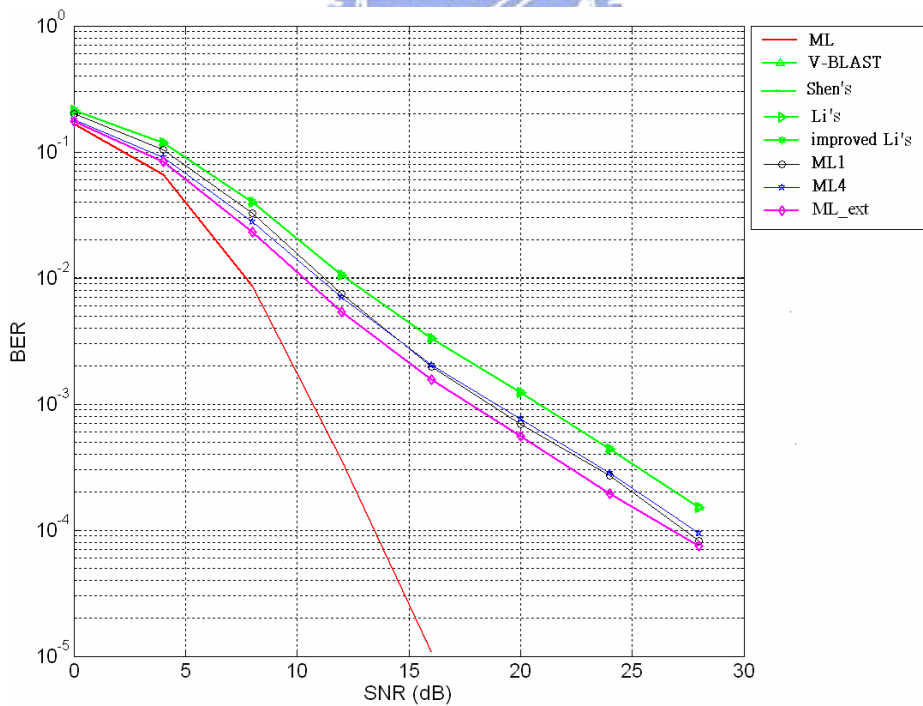


**Figure 4.10** BER performance versus SNR of various detection techniques (4x4), office environment

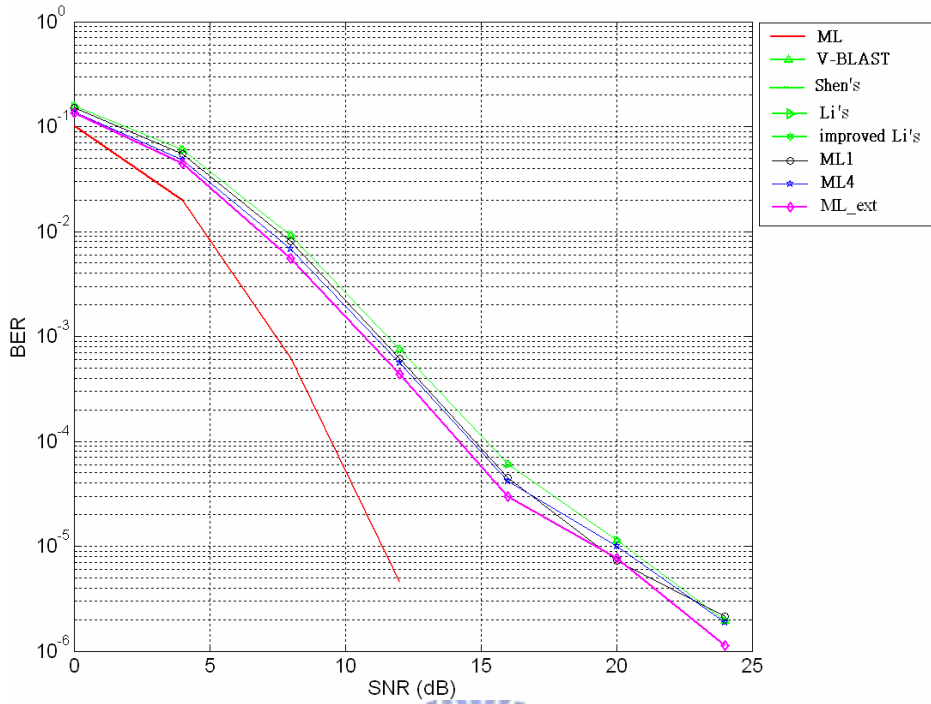


**Figure 4.11** BER performance versus SNR of various detection techniques (4x5), office environment

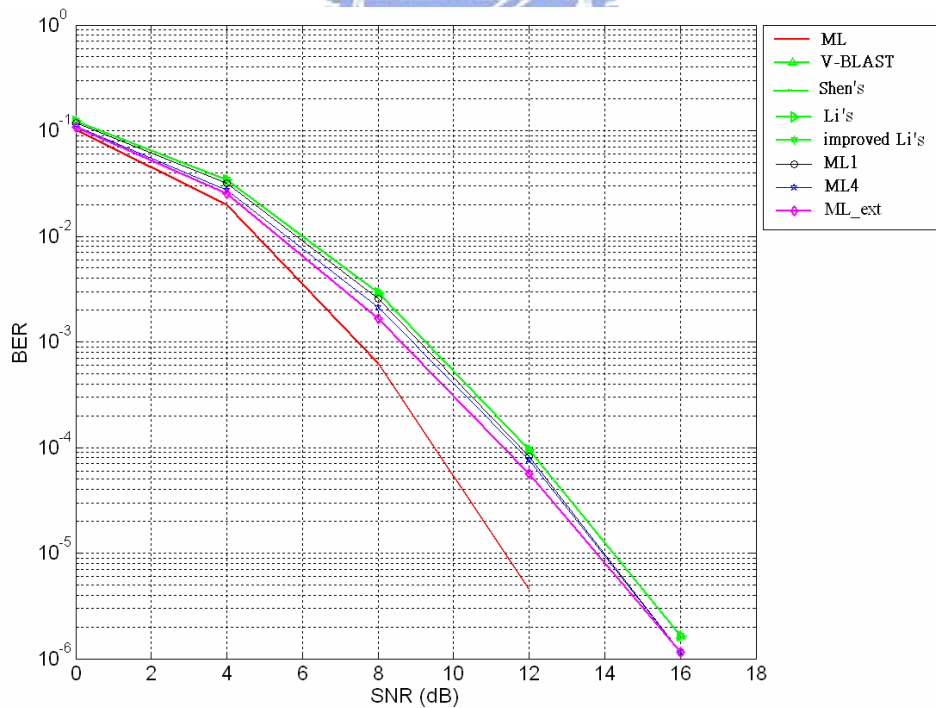


**Figure 4.12** BER performance versus SNR of various detection techniques (4x6), office environment

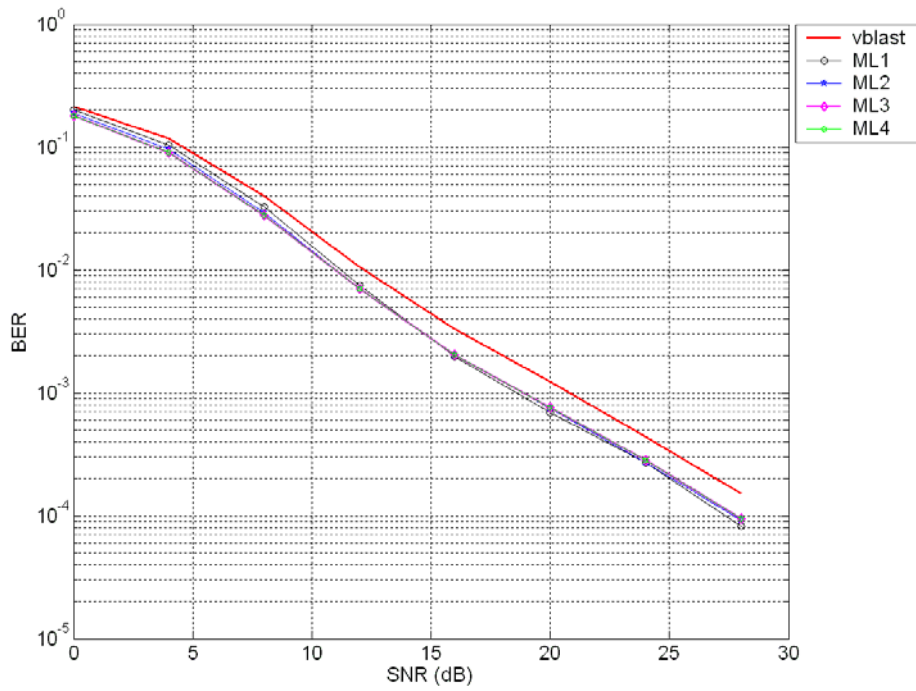


**Figure 4.13** BER performance versus SNR of our various detection techniques and V-BLAST (4x4), office environment

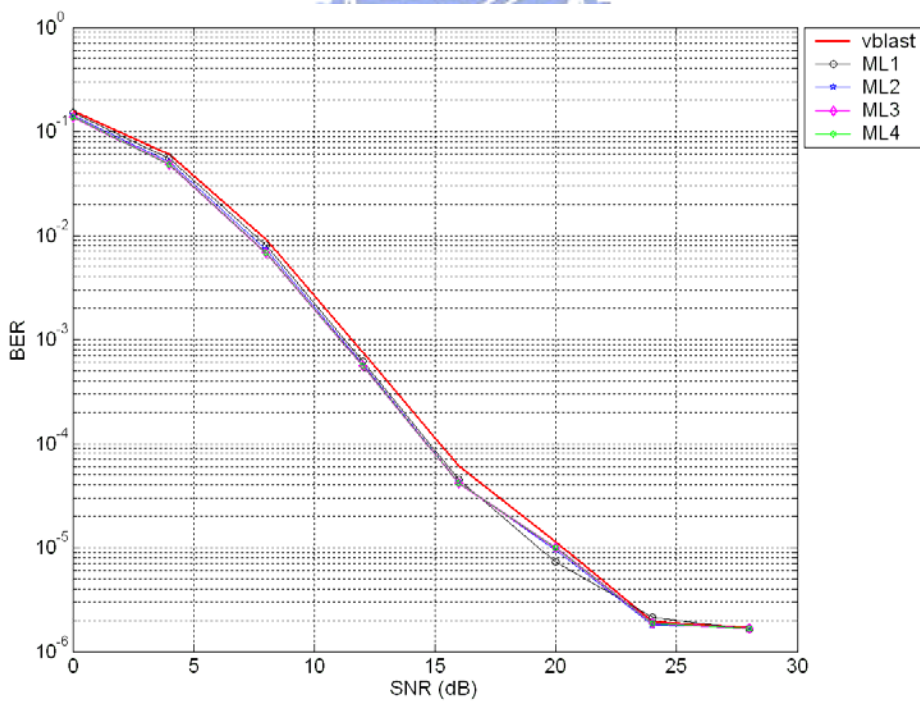


**Figure 4.14** BER performance versus SNR of our various detection techniques and V-BLAST (4x5), office environment

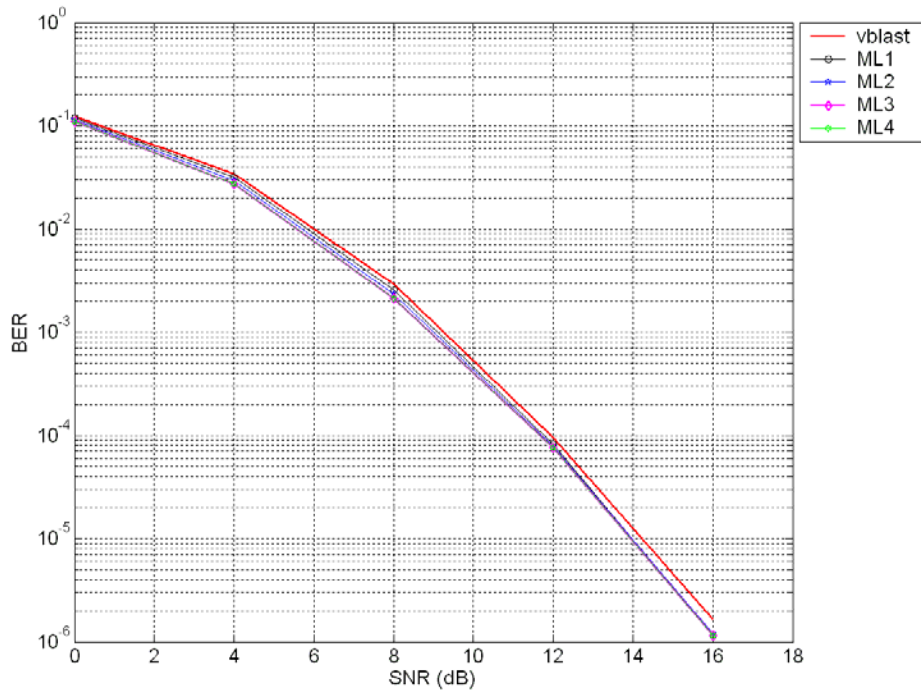


**Figure 4.15** BER performance versus SNR of the proposed detection techniques and V-BLAST (4x6), office environment

The second simulated channel is measured in an airport representing a typical large hall area. The channel has a few very long delay paths which indicate bad channel conditions and is harmful to communication. After simulation, the results in large hall are similar to results in office environment.

**Table 4.4** Indoor channel model [28], large hall environment

Tap No.	Delay (ns)	Power (dB)	Amplitude Distribution	Doppler Spectrum
1	0	0	Rayleigh	Classical
2	174	-8	Rayleigh	Classical
3	274	-15	Rayleigh	Classical
4	560	-18	Rayleigh	Classical

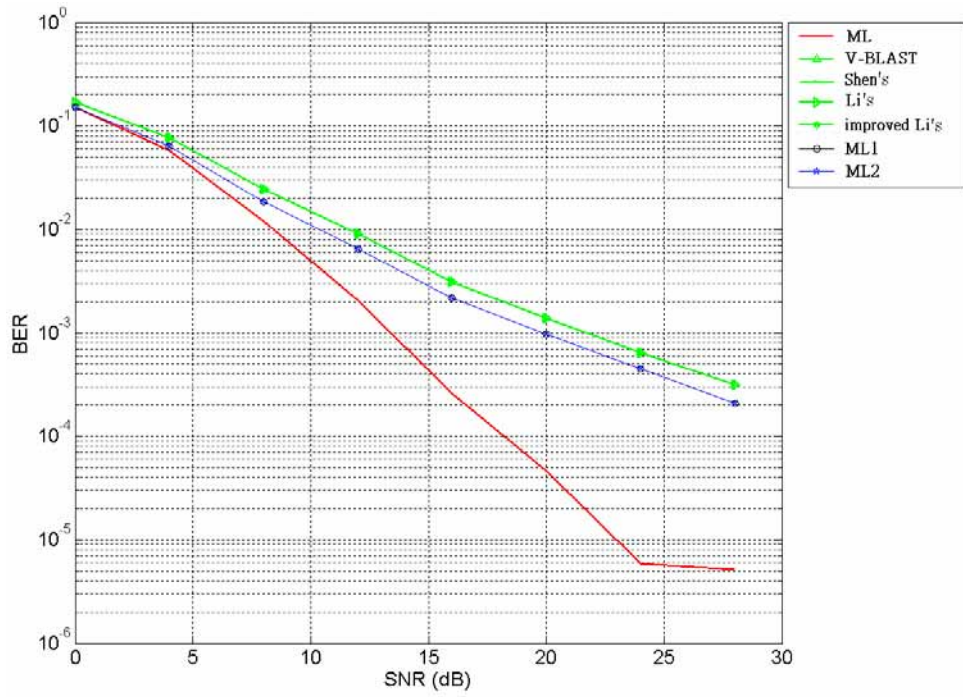


**Figure 4.16** BER performance versus SNR of various detection techniques (2x2), large hall environment

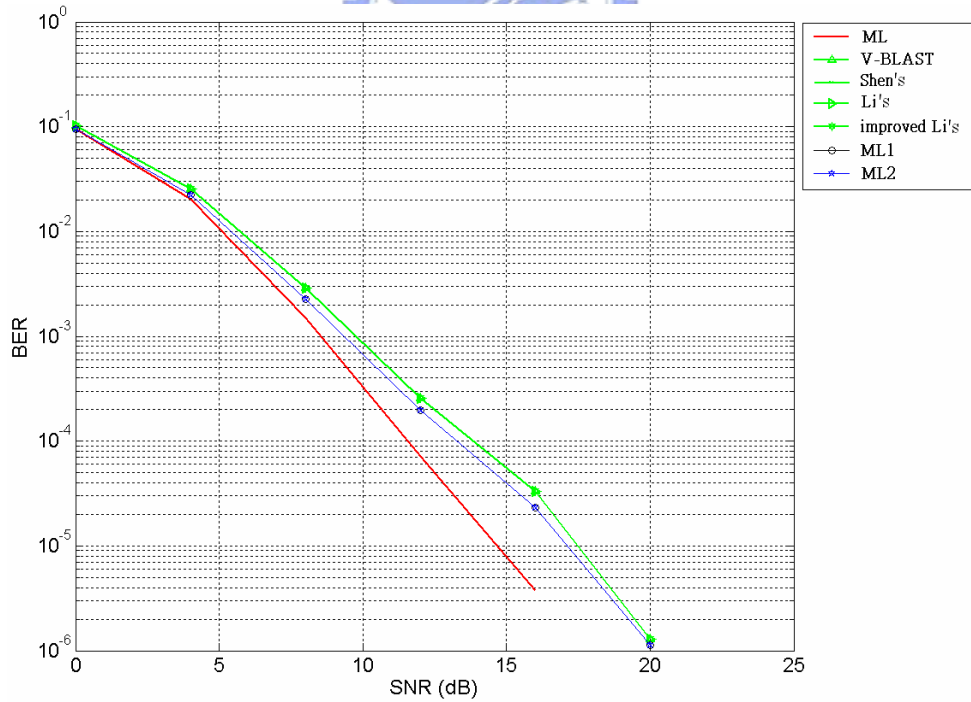


**Figure 4.17** BER performance versus SNR of various detection techniques (2x3), large hall environment

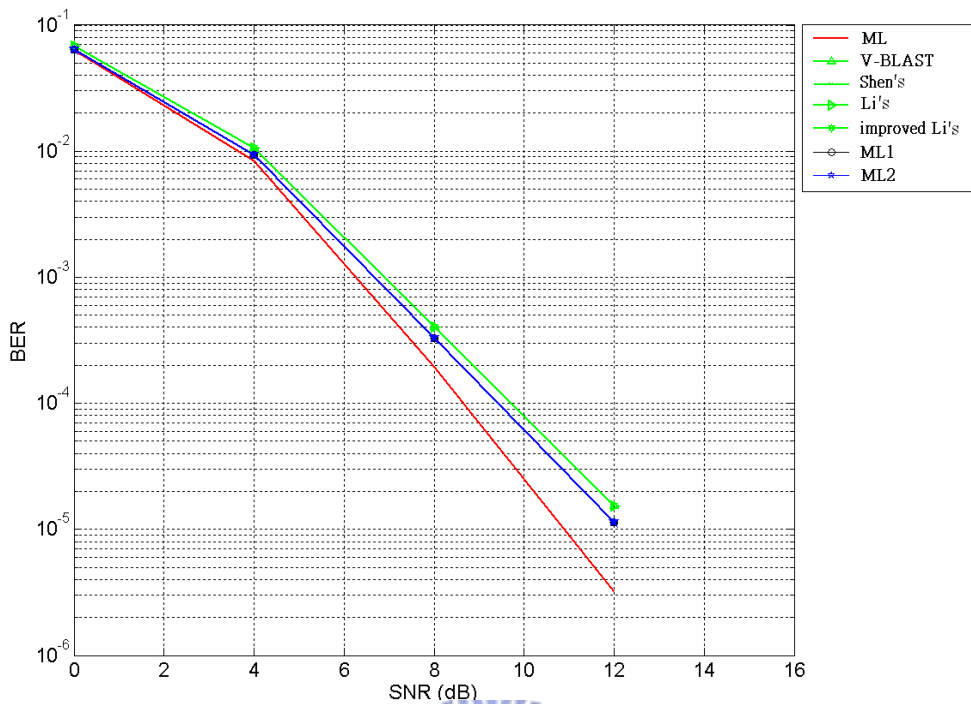


**Figure 4.18** BER performance versus SNR of various detection techniques (2x4), large hall environment

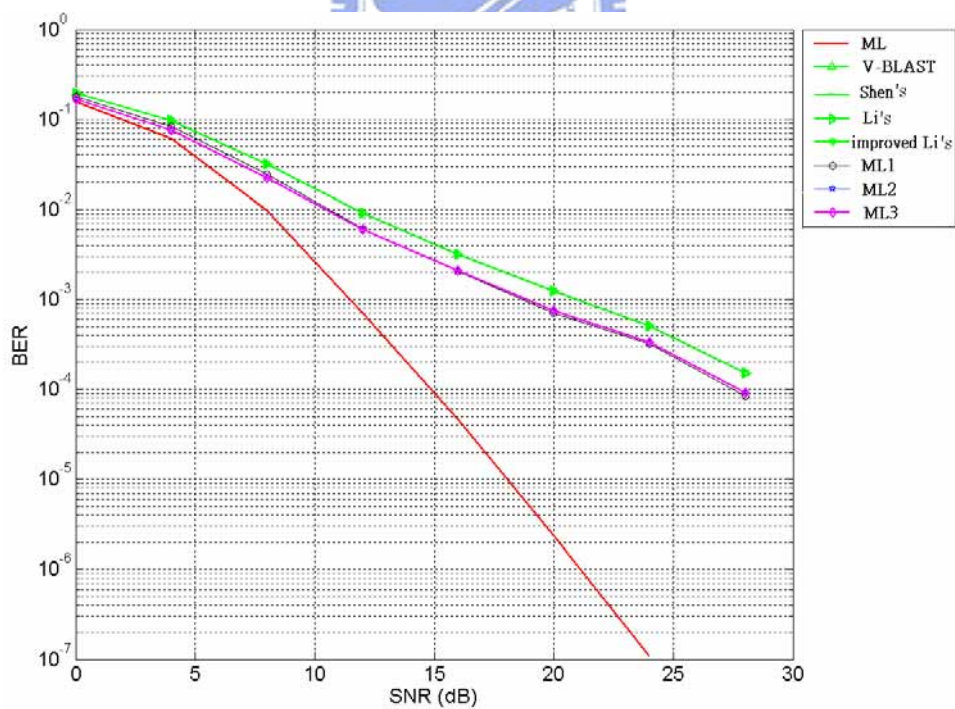


**Figure 4.19** BER performance versus SNR of various detection techniques (3x3), large hall environment



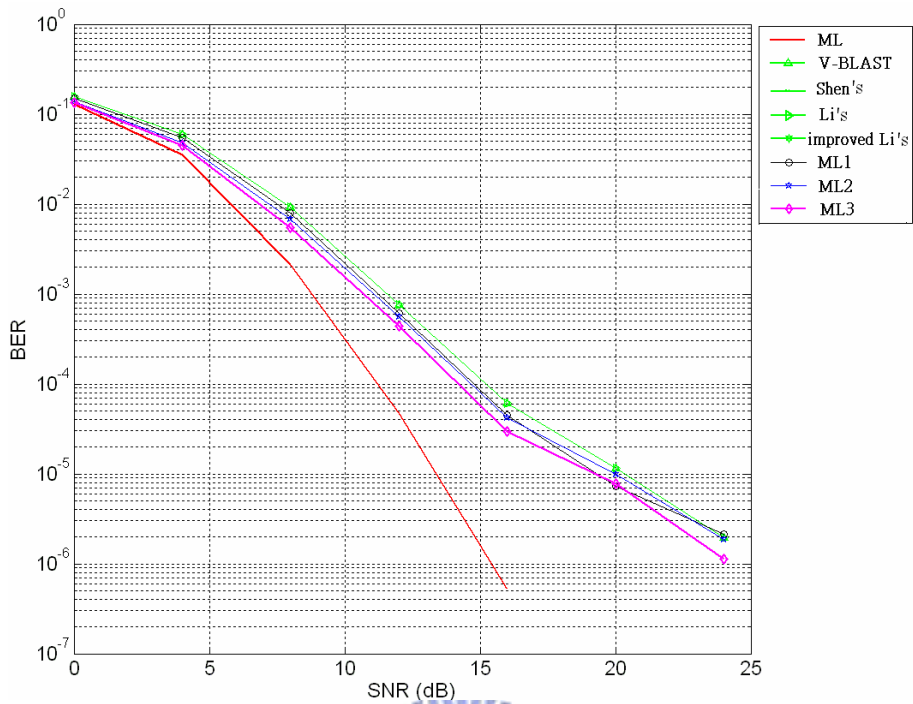


**Figure 4.20** BER performance versus SNR of various detection techniques (3x4), large hall environment

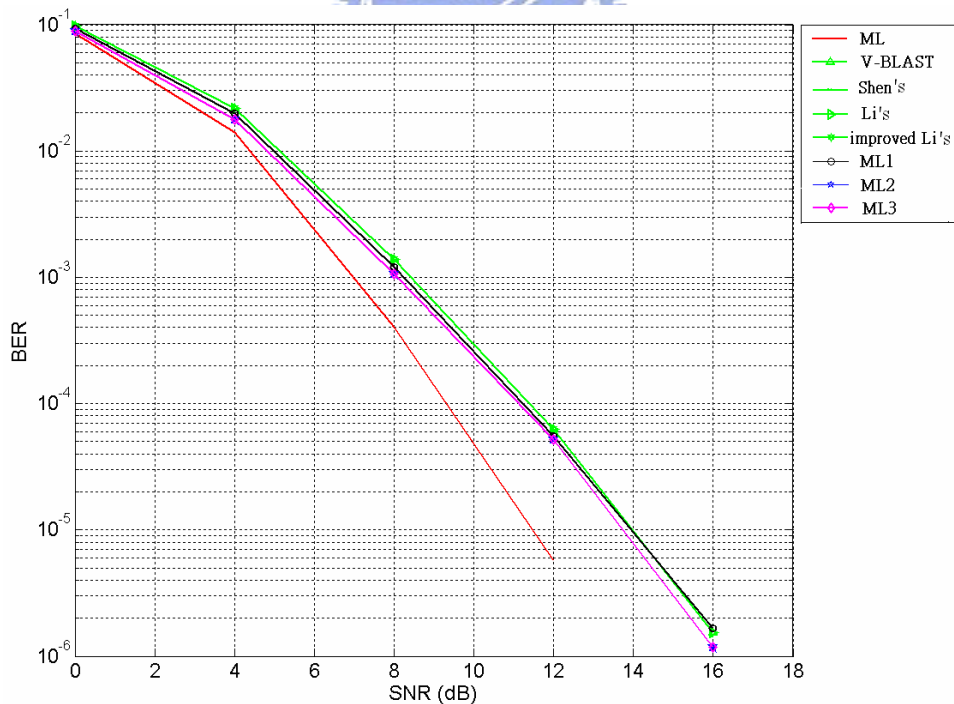


**Figure 4.21** BER performance versus SNR of various detection techniques (3x5), large hall environment

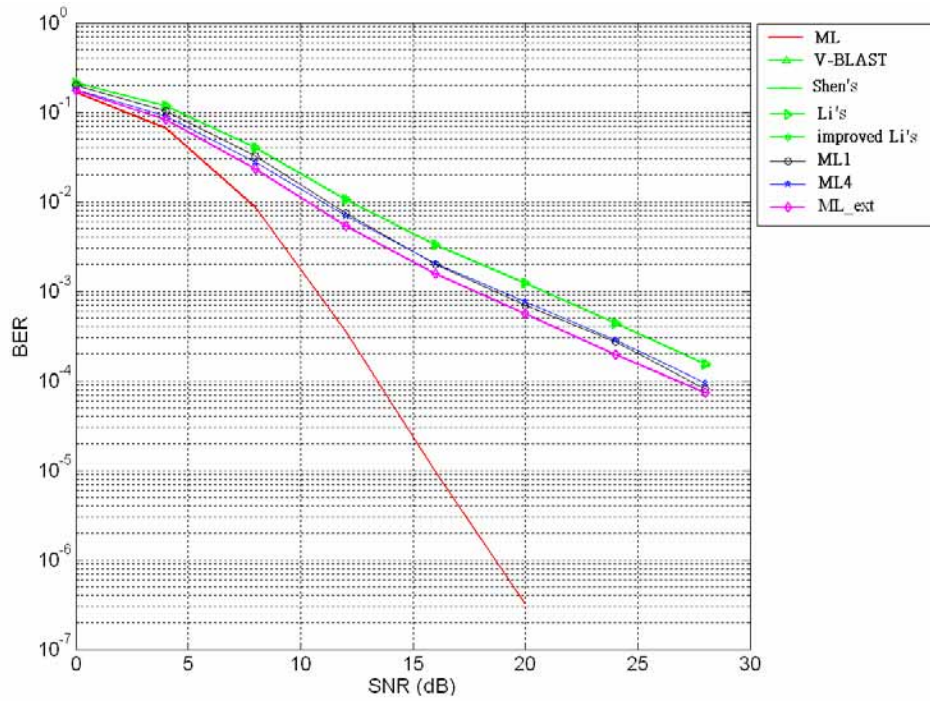


**Figure 4.22** BER performance versus SNR of various detection techniques (4x4), large hall environment

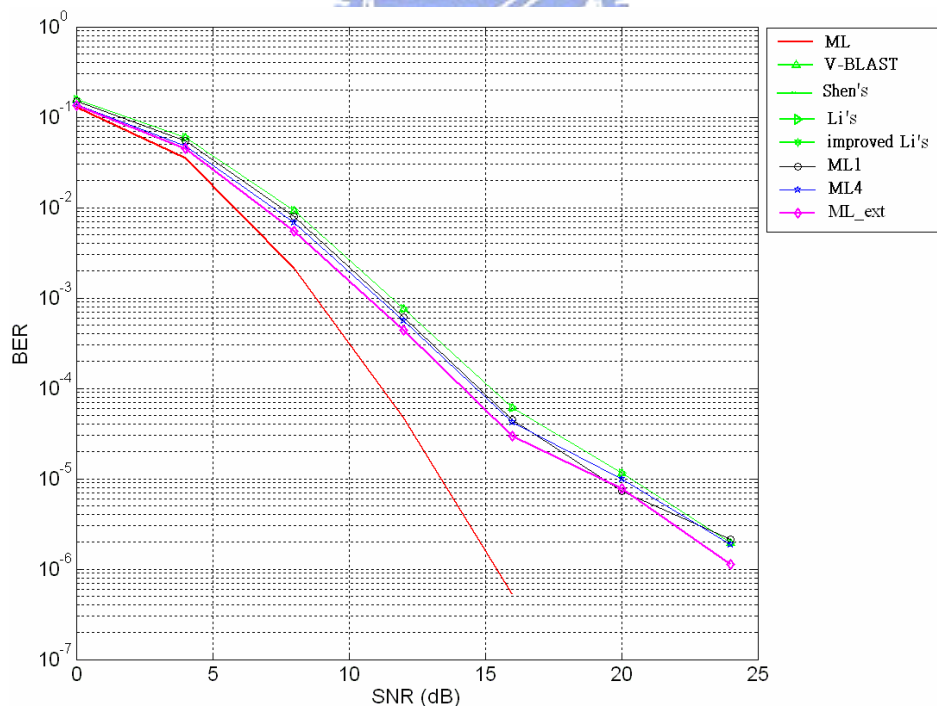


**Figure 4.23** BER performance versus SNR of various detection techniques (4x5), large hall environment



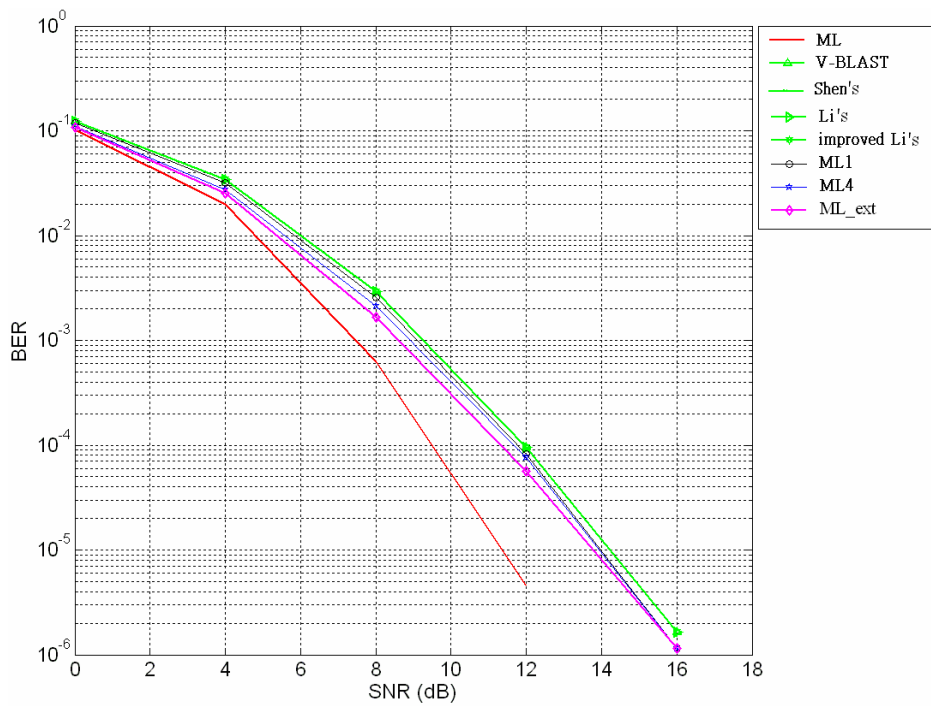


**Figure 4.24** BER performance versus SNR of various detection techniques (4x6), large hall environment

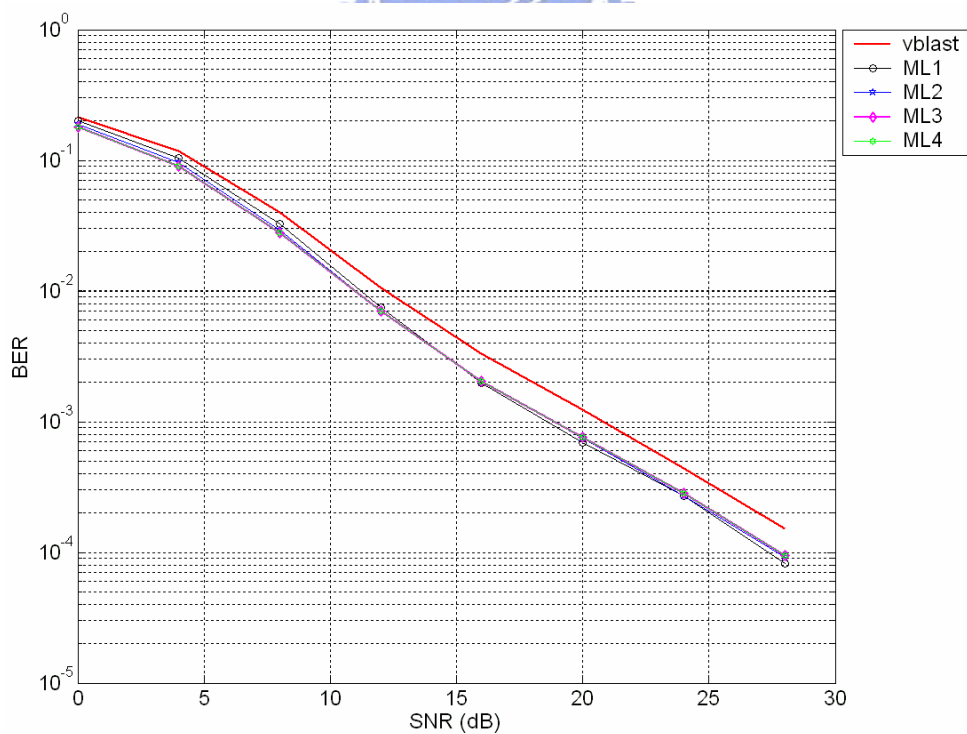


**Figure 4.25** BER performance versus SNR of the proposed detection techniques and V-BLAST (4x4), large hall environment

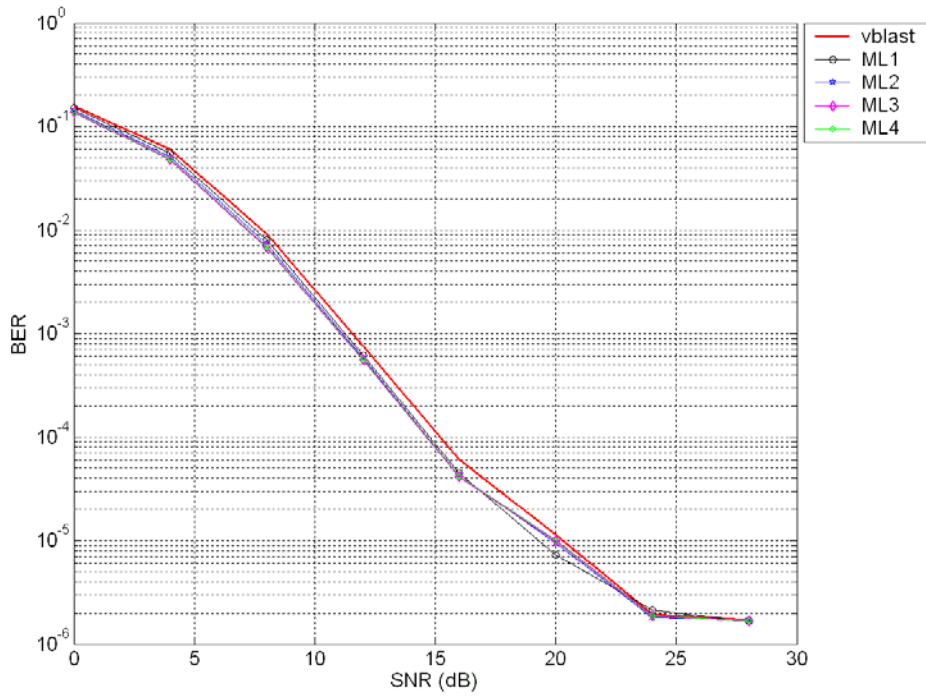


**Figure 4.26** BER performance versus SNR of the proposed detection techniques and V-BLAST (4x5), large hall environment

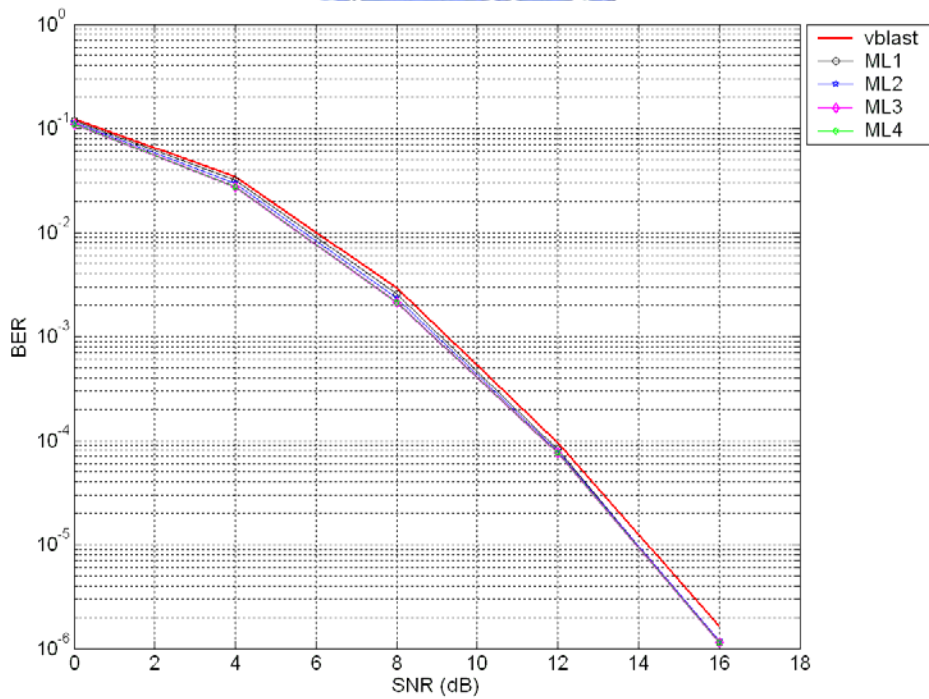


**Figure 4.27** BER performance versus SNR of the proposed detection techniques and V-BLAST (4x6), large hall environment



# Chapter 5

## Conclusion

In this thesis, many algorithms based on V-BLAST are introduced and simulated, and new algorithms for MIMO OFDM detection are proposed, followed by their investigations and verifications in terms of complexity and BER performance by testing EWC 802.11n systems. Although ML algorithm results in the best performance, it demands the highest computation cost. Therefore, we combine ML and V-BLAST methods, and reduce the complexity of ML detection by utilizing known detected values.

Since designs of detection methods are trade-off problems between cost and performance, complexity and performance analysis helps a lot to decide a suitable design. In complexity analysis, the proposed methods ( $L=1$ ) is roughly equal to V-BLAST method but its performance is better than V-BLAST method. Usually a detected layer will produce error and propagate to the following layers. The proposed methods have the better performance and less error propagation problem than other algorithm compare in the simulation. Testing 802.16e is considered as future work. It is also future work to reduce the complexity of pseudoinverse.

# Bibliography

- [1] T.Ojanpera and R. Prasad, "An overview of wireless broadband communications," IEEE Commun. Mag. Vol.35, No. 1, pp. 28-34, Jan 1997.
- [2] C. L.Ng, K. B. Letaief, and R.D. Murch, "Antenna diversity combining and finite-tap decision feedback equalization for high-speed data transmission," IEEE Journal on Selected Areas in Communication, Vol. 16, No.8, pp. 1367-1375, Qct. 1998.
- [3] B. Yang, K .B. Latief, R. S. Cheng, and Z. Cao, "Channel estimation for OFDM transmission in multipath fading channels based on parameter channel modeling," IEEE Transactions on Communications, Vol. 49, No. 3, March 2001.
- [4] W. K. Wang, R. S. Cheng, K. B. Latief, and R. D. Murch, "Adaptive antennas at the mobile and base station in an OFDM/TDMA systems," IEEE Transactions on Communications, Vol. 49, No.1, Jan. 2001.
- [5] C. Y. Yue, R. S. Cheng, K. B. Letaief, and R. D. Murch, " Multiuser OFDM with subcarrier, bit, and power allocation," IEEE Journal on Selected Areas in Communications, Vol. 17, No. 10, pp. 1747-1758, October 1999.
- [6] G. J. Foschini and M. J. Cans, "On limits of wireless communications in a fading environment when using multiple antennas," Wireless Personal Communications, Vol. 6, NO. 3, pp. 311-335, 1998.
- [7] G. G. Raleigh and J. M. Cioffi, "Spatio-temporal coding for wireless communication," IEEE Trans. Communications, Vol. 46, No. 3, pp. 357-366, March 1998.
- [8] G. J. Foschini, "Layered space-time architecture for wireless communication in a fading environment when using multiple antennas," Bell laboratories Technical Journul, Vol. 1, No. 2, pp. 41-59, 1996.
- [9] P. W. Wolniansky, G. J. Foschini, G. D. Golden, R. A. Valenzuela, "V-BLAST an architecture for realizing very high data rates over the rich-scattering wireless channel," Invited paper; Proc. ISSSE-98, Pisa, Italy, 1998.
- [10] N. Boubaker, K. B. Letaief, and R. D. Murch, "A layered space-time coded wideband OFDM architecture for dispersive wireless links," Computers and Communications, 2001, Proceedings, Page(s): 518 – 523, July 2001

- [11] <http://www.enhancedwirelessconsortium.org/home>
- [12] IEEE Std 802.11a-1999, Wireless LAN Medium Access Control (MAC) and Physical Layer (PHY) Specifications, 1999 edition.
- [13] N. Boubaker, K. B. Letaief, R. D. Murch, "A low complexity multicarrier BLAST architecture for realizing high data rates over dispersive fading channels," VTC 2001 Spring, IEEE VTS 53<sup>rd</sup> Volume 2, Page(s): 800 - 804 vol.2, 6-9 May 2001.
- [14] Y. Li, J.C. Chuang and N.R. Sollenberger, "Transmitter diversity for OFDM systems and its impact high rate data wireless networks," IEEE Journal on Selected Areas in Communications, Vol. 17, NO. 7, pp. 1233-1243, July 1999.
- [15] S.B. Bulumulla, S.A. Kassam and S.S. Venkatesh, "An adaptive diversity receiver for OFDM in fading channels," IEEE Conference on Communications 88, Proc. 1998, Vol. 3, pp. 1325-1329.
- [16] G. Yi and K. B. Letaief, "Performance evaluation and analysis of space-time coding in unequalized multipath fading links," IEEE Transactions on Communications, Vol. 48, pp. 1778-1782, Nov. 2000.
- [17] J.J. Wang and Ta-Sung Lee, "Applications of dynamic subcarrier allocation and adaptive modulation in multiuser MIMO-OFDM systems" Master thesis, Institute of Communication Engineering, Hsinchu, Taiwan, National Chiao Tung University, 2004.
- [18] G.Y. Lin and S.G. Chen, "On signal Detection of MIMO OFDM Systems" Master thesis, Institute of Electronics College of Electrical Engineering, Hsinchu, Taiwan, National Chiao Tung University, 2004.
- [19] C. Shen, H. Zhuang, L. Dai, S. Zhou, and Y. Yao, "Performance Improvement of V-BLAST through an Iterative Approach," Personal, Indoor and Mobile Radio Communications, 2003. PIMRC 2003. 14th IEEE Proceedings , Vol. 3, pp. 2553 - 2557, Sept. 2003.
- [20] Q. Liu, and L. Yang, "A simplified method for V-BLAST detection in MIMO OFDM communication," Communications, 2004 and the 5th International Symposium on Multi-Dimensional Mobile Communications Proceedings. The 2004 Joint Conference of the 10th Asia-Pacific Conference on Volume 1, 29 Aug.-1 Sept. 2004 Page(s): 30 - 33 vol.1.

- [21] D. Li, L. Cai, and H. Yang, "New iterative detection algorithm for V-BLAST," IEEE Conference on Vehicular Technology Conference, Vol. 4, pp. 2444 - 2448, Sept. 2004.
- [22] J. Akhtar "Enhanced detection for zero-forced V-BLAST," IEEE Conference on Vehicular Technology Conference, Vol. 2, pp. 848 - 852, May 2004.
- [23] S. Baro, G. Bauch, A Pavlic, and A. Semmler, "Improving BLAST performance using space-time block codes and turbo decoding," IEEE Conference on Global Telecommunications, Vol. 2, pp. 1067 - 1071, Nov. 2000.
- [24] G.D. Golden, C.J Foschini, R.A. Valenzuela, and P.W. Wolniansky, "Detection algorithm and initial laboratory results using V-BLAST space-time communication architecture," Electronics Letters, Vol. 35, pp. 14-16, Jan. 1999
- [25] T.Q. Duong, E.K. Hong, and S.Y. Lee, "Effect of the Modified Channel Matrix on the MMSE V-BLAST System Performance" IEEE Conference on Wireless And Mobile Computing, Networking And Communications, Vol. 1, pp. 133-136, Jan. 2005
- [26] T. Xiaofeng, C.Elena, Y. Zhuizhuan, Q. Haiyan and Z. Ping "New detection algorithm of V-BLAST space-time code," IEEE Conference on Vehicular Technology Conference, Vol. 4, pp. 2421 - 2423, Oct. 2001.
- [27] I.N. Herstein and D.J. Winter, Matrix Theory and Linear Algebra, 1st ed, Macmillan Publishing Co. 1988
- [28] X. Zhao, J. Kivinen, and P. Vainnikainen, "Tapped delay line channel models at 5.3 GHz in indoor environments," Vehicular Technology Conference, 2000. IEEE VTS-Fall VTC 2000. 52nd Volume 1, 24-28 Sept. 2000 Page(s): 1 – 5 vol.1.